SEDIMENTOLOGY the journal of the International Association of Sedimentologists

Sedimentology (2022) **69**, 2779–2813 doi: 10.1111/sed.13017

Variability in fluvially-dominated, fine-grained, shallow-water deltas

ANTONY DAVID REYNOLDS
Department of Geology and Petroleum Geology, University of Aberdeen, Meston Building, Aberdeen, Scotland, AB24 3UE,UK (E-mail: paralic.reservoirs@gmail.com)

Associate Editor – Jeff Peakall

ABSTRACT

Fluvially-dominated, fine-grained, shallow-water deltas are more variable than is generally recognized. Studies of the Mississippi River imply rather persistent river-mouth jet dynamics, resulting in either progressive channel bifurcation around middle-ground mouth bars on lobate deltas, or steady channel progradation to form elongate deltas akin to the modern Mississippi Delta. By contrast, satellite imagery and historical maps of less well-known fluvially-dominated deltas show diverse river-mouth deposits, with planform shapes ranging from river-mouth fans, through splay, triangular, frond and tongue-shaped mouth bars, to elongate channels with prominent subaqueous levées. Critically, such deposits may vary along individual channels and across or between individual lobes suggesting that jet variability can be normal, and that a spectrum of jets forms a suite of stable river-mouth deposits. Channel elongation can also be common. In addition to high-inertia jets and delta-head or backwater-mediated avulsion, two further mechanisms are recognized to form elongate channels. Following channel splitting, dominant splits can shoulder aside mouth bars, so that subordinate splits wither and dominant splits extend the parent channel. Alternatively, river-mouth fans, subordinate distributary networks and lobes may be abandoned, so that a dominant parent distributary is rejuvenated by receiving an increase in discharge, allowing progradation to continue. Individual real-world deltas are expected to be characterized by a range of river-mouth deposits, both laterally and over time. However, such variable river-mouth deposits, and different modes of channel elongation, are not generally considered in models of fluvially-dominated deltas – omissions that may have significant impact for land remediation projects on modern deltas, and descriptions of the subsurface constructed to aid resource extraction.

Keywords Delta lobes, distributary channel elongation, fluvially-dominated, mouth bars, river-mouth deposits.

INTRODUCTION

Deltas are home to 4% of the world's population (Edmonds *et al.*, 2020), are important sites for agriculture (Schneider & Asch, 2020) and fisheries (Lauria *et al.*, 2018; Loucks, 2019), and are under threat from the combined impacts of subsidence (Syvitski, 2008; Syvitski *et al.*, 2009; Higgins, 2016), reduced sediment supply (Giosan *et al.*, 2014) and sea-level rise (Ericson *et al.*, 2006). As a result, they are the focus of intervention strategies and projects to mitigate or reverse land loss (Haasnoot *et al.*, 2012; Giosan *et al.*, 2014; Lwasa, 2015; Tessler *et al.*, 2015; LACPRA, 2017; Bergillos *et al.*, 2018; Bomer *et al.*, 2019). Deltaic sediments are also important in the subsurface

where they act as aquifers (Ahmed *et al.*, 2004; Custodio, 2010; Scheelbeek *et al.*, 2017; Abd-Elaty *et al.*, 2019), contain coal deposits (Whateley & Pickering, 1989) and form petroleum traps (Hampson *et al.*, 2017; Reynolds, 2017). To optimize the extraction and management of these resources, and to ensure the success of interventions on modern systems, it is critical to understand the variability of deltaic systems, and to be able to robustly model them.

Variability within deltaic systems is generally described in terms of the relative influence of fluvial and basin processes, typically waves and tides (Galloway, 1975; Giosan *et al.*, 2005; Ainsworth *et al.*, 2011) but also storms (Lin & Bhattacharya, 2021), each of which may vary locally, and through time, in particular with sea-level change (Reynolds, 1996). Here, however, the focus is on exploring the short-term variability of shallow-water, fine-grained, fluvially-dominated deltas where basin processes have minimal impact. Fisher (1969) described two types of fluvially-dominated deltas. Elongate deltas, as typified by the modern-day Mississippi Delta, are characterized by an elongate plan form with unfilled accommodation space at the delta margin, and a limited number of elongate, rarely-branching distributary channels (Kim *et al.*, 2009). By contrast, lobate deltas, exemplified by the Holocene Lafourche, St. Bernard and Teche deltas of the Mississippi River, are marked by a lobate plan form and a semi-radial spray of distributary channels that progressively split and narrow across the delta plain. Though the difficulties of distinguishing between elongate trunk channels and incised valleys in the subsurface has been noted, and a preponderance of lobate river-dominated, shallow-water deltas has been suggested (Olariu & Bhattacharya, 2006), both delta types continue to be recognized as important end members. Furthermore, they are increasingly well-understood in terms of river-mouth jet dynamics (Canestrelli *et al.*, 2014; Fagherazzi *et al.*, 2015), with lobate deltas being formed when lower-inertia jets deposit middle-ground mouth bars that force progressive channel splitting as progradation proceeds, 'a bifurcation driven model' (Edmonds & Slingerland, 2007; Jerolmack & Swenson, 2007; Jerolmack, 2009) and elongate deltas developing when higher-inertia jets form elongate subaqueous levées and foster channel elongation rather than splitting (Rowland *et al.*, 2005; Kim *et al.*, 2009; Rowland *et al.*, 2009, 2010).

In general though, with the exception of the longstanding recognition that trunk channels of elongate deltas may be fringed by crevasse deltas that are small-scale examples of lobate deltas (Coleman & Gagliano, 1964; Olariu & Bhattacharya, 2006), descriptions of river-dominated systems have tended to infer a single style of delta, and by inference a rather persistent form of river-mouth jet that deposits a single style of river-mouth deposit. For example, high-quality, well-known studies of crevasse and bay-head deltas of the Mississippi system have been described in terms of self-similar, middle-ground mouth bars and terminal channels (Welder, 1955; Van Heerden & Roberts, 1988; Wellner *et al.*, 2005; Olariu & Bhattacharya, 2006). Many ancient systems have been interpreted similarly: lobate deltas characterized by friction-dominated mouth bars are widely recognized (Flint *et al.*, 1989; Harris, 1989; Tye & Hickey, 2001; Olariu & Bhattacharya, 2006; Turner & Tester, 2006), and several systems are considered analogous to the bar-finger sands of the modern-day Mississippi Delta (Elliott, 1976; Okazaki & Masuda, 1989; Pulham, 1989). By contrast, more recent outcrop studies suggest that diverse channel-termination processes and depositional elements can co-exist, such as: (i) coeval, proximal, friction-dominated mouth-bar deposits, and distal, inertia-dominated hyperpycnal deposits (Ahmed *et al.*, 2014; Jerrett *et al.*, 2016); (ii) lunate, high-inertia mouth bars lain down during high stage, which divert low-stage flows to form marginal, smaller, friction-dominated mouth bars (Fidolini & Ghinassi, 2016); and (iii) an evolution that commences with a jet which fills the water column, deposits on the centreline and drives dunes basinward down low-angle foresets, but which detaches from the bar front (as aggradation occurs and water depth increases) to form an avalanche foreset (Cole *et al.*, 2020).

Case studies presented here bolster this view of river mouth diversity. An expanded range of river-mouth deposits is illustrated, including a complex suite of mouth-bar forms. Together they suggest short-term, river-mouth jet variability, along individual channels, between adjacent channels and across delta lobes. Furthermore, additional modes of channel extension are documented, which are hypothesized to maintain larger channels, and result in longer delta lobes. Though some of this variability has been hinted at by numerical models and flume experiments that mimic river mouths, real world examples have not been previously highlighted, and the diversity of forms is, as yet, not integrated in to a coherent model at the delta lobe and delta scale.

To provide a framework for the case studies the paper commences with summaries of the bifurcation-driven model and controls on river-mouth deposits, but it focusses on subsequent sections which illustrate diversity in channel-mouth deposits and variable modes of channel elongation. The examples, some that have been extensively studied in the past, and others newly accessed through historical satellite imagery, are drawn from systems that range from 2 to 220 km in width, and include complete deltas and sub-deltas of larger systems (such as the Mississippi Delta; Table 1). The deltas prograde in to water depths that range from 2 m to over 25 m, and are mostly from lacustrine and bay settings. The grain size of the discussed depositional elements ranges from fine sand to coarse silt (Table 1).

THE BIFURCATION-DRIVEN MODEL FOR FLUVIALLY-DOMINATED DELTAS

As river-dominated delta lobes prograde, mouth-bar deposition and channel bifurcation can lead to an increasing number of narrower, shorter channels and smaller mouth bars with distance from the delta apex (Olariu & Bhattacharya, 2006; Jerolmack & Swenson, 2007; Jerolmack, 2009; Wolinsky *et al.*, 2010; Edmonds *et al.*, 2011; Fig. 1A and B). Diverse studies have quantified this bifurcation-driven model.

1 A weak correlation exists between channel segment length (L) and channel width (W) (Edmonds *et al.*, 2004) with $L = \sim 10W$ (Jerolmack & Swenson, 2007; Jerolmack, 2009).

2 On average, channels diverge at an angle of 72° (Coffey & Shaw, 2017).

3 Mouth-bar crests tend to stabilize at a distance of three to four channel widths from the channel mouth ($L_B = W_0 \times 3$ to 4; Fig. 1Aii) (Wright & Coleman, 1974; Edmonds & Slingerland, 2007; Fig. 1C).

4 Widths of daughter channels (W_1 and W_2, Fig. 1Aii) are typically unequal with a width ratio of around 1.7 (Edmonds & Slingerland, 2007).

5 Successive channel segment widths and lengths decrease by a factor of around 0.7 (Edmonds & Slingerland, 2007; Jerolmack, 2009; Fig. 1D). The resulting channel pattern (Fig. 1Bi) is similar at different scales, and has been described (Jerolmack & Swenson, 2007; Jerolmack, 2009) and shown mathematically to be fractal on modern, numerical, theoretical and experimental deltas (Seybold *et al.*, 2007; Wolinsky *et al.*, 2010; Edmonds *et al.*, 2011).

6 The decrease in channel-segment length at each split limits lobe growth, and at the same time a growing wetted-channel perimeter increases bed friction (Fig. 2). Both factors increasingly make the growing lobe a barrier to progradation and onward flow, and favour avulsion.

7 Rare, anomalously-long channel segments are considered to be the product of avulsion which is most likely to occur at the backwater length (the point at which the river bed descends below sea or lake level, and where the river begins to feel the influence of the standing body of water; Jerolmack & Swenson, 2007) or at the delta head (Hartley *et al.*, 2017; Fig. 1 B(iii)).

The bifurcation-driven model, and in particular its quantification, forms a cornerstone of the understanding of lobate fluvially-dominated deltaic systems. Subsequent studies have extended the modelling on which it was based and emphasized features that it does not fully describe, such as alternate modes of avulsion forced by morphodynamic autogenic behaviour (Edmonds *et al.*, 2009; Hoyal & Sheets, 2009; Rosa *et al.*, 2016), and prolonged elongation of distributary channels by river mouth jets (Rowland *et al.*, 2005, 2009; Kim *et al.*, 2009). The examples presented below continue that trend by illustrating diverse river-mouth deposit styles, and a range of channel elongation mechanisms.

RIVER-MOUTH DEPOSITS

River-mouth deposits are perhaps the key elements of fluvially-dominated delta lobes. Synthesizing studies of modern deltas, Wright (1977) described three idealized river-mouth deposits: friction, inertia and buoyancy-dominated mouth bars. Friction-dominated examples display triangular, 'middle-ground', channel-mouth bars (Welder, 1955; Belevich, 1956; Axelsson, 1967; Van Heerden & Roberts, 1988; Fielding *et al.*, 2005; Wellner *et al.*, 2005). The bars split the parent channel, forcing the basinward reduction in channel and bar dimensions fundamental to the bifurcation-driven model. Wright (1977) viewed inertia-dominated deposits to be: (i) favoured by channels that debouch in to relatively deepwater, so that the channel-mouth jet expands in three dimensions; and (ii) rare and

Table 1. Examples of diverse river mouth deposit styles and elongate channels from fluvially-dominated deltas. In general, the examples developed in shallow water depths, <2 to 25 m, and the grain size of depositional elements of interest ranges from silt to fine sand. Many case studies display more than one style of river-mouth deposit.

Location	Depositional element (widths given for underlined elements)	Setting	Age	Water depth (m)	Element width (km)	Grain size	Location	Examples in this paper	Timescale of example (years)	References
Volga Delta, Russia	Delta composed of elongate sub-deltas and lobes	Lacustrine	Modern	<2–3	220	~90 μm in levées and channels	45°47′13.73″N 47°54′56.58″E	Figs 14 and 15	152	Overeem *et al.* (2003)
Songliao Basin, China	Delta composed of elongate sub-deltas and lobes	Lacustrine	Upper Cretaceous	–	>18	Fine sand and silt (medium grained at channel bases)	46°39′34.51″N 124°32′33.39″E	Fig. 17		Zeng *et al.* (2013)
Mississippi Bird Foot Delta, USA	Bird foot delta	Marine	Modern	>3000	48	Fine to very fine sand mouth bars	29° 8′48.71″N 89°15′5.56″W			Fisk (1961); Wright & Coleman (1974)
Omo Delta, Ethiopia/ Kenya, East Africa	Delta with elongate channels, high-friction fan, middle-ground bars	Lacustrine	Modern	<5	31	60-200 μm adjacent to channels	4°26′38.51″N 35°59′13.39″E	Fig. 7	16	Butzer (1970); Velpuri *et al.* (2012); Carr (2017)
St Clair Delta, Canada and USA	Delta with elongate channels	Lacustrine	Modern	6	30	Very fine sand and coarse silt	42°34′30.39″N 82°36′10.77″W			Pezzetta (1973)
Catatumbo Delta, Lake Maracaibo, Venezuela	Delta with elongate channels and middle ground bars	Lacustrine	Modern	25	16	Fine lower to coarse silt mouth bars	9°20′17.86″N 71°46′10.16″W	Fig. 6	43	Hyne *et al.* (1979)
Sarygamysh Lake, Turkmenistan	Delta with river mouth fan and elongate channels	Lacustrine	Modern	–	10	–	42° 3′47.38″N 57°39′26.21″E			
Mossy Delta, Saskatchewan, Canada	Delta with middle ground bars and elongate channel	Lacustrine	Modern	12	6	D50 125 μm	54° 4′9.57″N 102°22′59.00″W	Fig. 11	35	Edmonds & Slingerland (2007); Caldwell & Edmonds (2014)
Red River Delta, Lake Texoma, Texas	Delta with fan, frond, middle ground and tongue river mouth deposits	Lacustrine	Modern	9	2	Suspended sediment in the channel has median values of fine silt (8 μm) to very fine sand (125 μm)	33°56′40.20″N 96°54′5.23″W	Fig. 5	44	Olariu *et al.* (2012); Huling & Holbrook (2016); Howe (2017)
Cubit's Gap Crevasse Delta, Mississippi, USA	Crevasse delta with elongate channels, middle ground bars	Marine	Modern	>9	18	Mouth bar sands ~125 μm	29°11′45.45″N 89°15′49.01″W	Fig. 8	90	Welder (1955); Cahoon *et al.* (2011); Esposito *et al.* (2013)
Atchafalaya Delta, Mississippi, USA	Bay head delta composed of middle ground mouth bars	Marine	Modern	2	12	Fine sand, silt, and clay	29°27′52.47″N 91°16′46.72″W	Fig. 9	41	Van Heerden & Roberts (1988); Van Heerden *et al.* (1991); Roberts (1998)

Table 1. (continued)

Location	Depositional element (widths given for underlined elements)	Setting	Age	Water depth (m)	Element width (km)	Grain size	Location	Examples in this paper	Timescale of example (years)	References
Wax Lake Delta, Mississippi, USA	Bay head delta composed of middle ground mouth bars	Marine	Modern	2	12	Mouth bar D50 5–80 μm	29°31′53.33″N 91°26′4.24″W	Fig. 12	61	Wellner *et al.* (2005); Shaw & Mohrig (2014)
Volga Delta, Russia	Minor delta lobe with tongue, frond, and terminal splay mouth bars	Lacustrine	Modern	<2–3	1.2	~90 μm levées and channels	45°41′7.99″N 48°11′44.32″E	Fig. 4	2	Overeem *et al.* (2003)
Valdarno Basin, Italy	Tongue and terminal splay mouth bars	Lacustrine	Pliocene	–	6–15 m	Very coarse to very fine sand	43°34′48.93″N 11°27′24.63″E			Fidolini & Ghinassi (2016)
Mississippi River elongate channel, Mississippi, USA	Elongate channel	Marine	Modern	<9	4	–	29°22′46.15″N 89°33′2.54″W			Kim *et al.* (2009)
Gilgal Abay Delta, Lake Tana, Ethiopia	Elongate channel	Lacustrine	Modern	12	2	–	11°51′1.94″N 37° 8′15.50″E			Kim *et al.* (2009); Wale (2008)
Lake Lewisville, Texas, USA	Elongate channel	Lacustrine	Modern	4	0.6	–	33°12′48.69″N 97°1′57.44″W			Huling & Holbrook (2016)
Lake Kemp, Texas, USA	Elongate channel	Lacustrine	Modern	6	0.35	–	33°44′13.51″N 99°14′33.01″W			Huling & Holbrook (2016)
Grapevine Reservoir, Texas, USA	Elongate channel	Lacustrine	Modern	5	0.4	Sand in channels. Sand and silt on levées	33°1′33.93″N 97°9′47.51″W			Tomanka (2013); Howe (2017)
Raccourci Old River, Lower Mississippi River, USA	Elongate channel	Oxbow lake	Modern	–	0.5	Levée D50 96 μm (coarse layer), mouth bar D50 292 μm	30°52′42.23″N 91°33′49.00″W			Rowland *et al.* (2005); Rowland (2007); Rowland *et al.* (2010)
414TC Fly River, Indonesia and Papua New Guinea	Elongate channel		Modern	–	0.15	Levée D50 45 μm	6°16′38.33″S 141°2′17.69″E			
346TC Fly River, Indonesia and Papua New Guinea	Elongate channel		Modern	–	0.12	Levée D50 44 μm	6°43′7.24″S 140°52′53.44″E			
Birch Creek, Alaska, USA	Elongate channel		Modern	–	0.05	Levée D50 60 μm, mouth bar D50 200 μm	65°53′41.63″N 144°18′10.88″W			

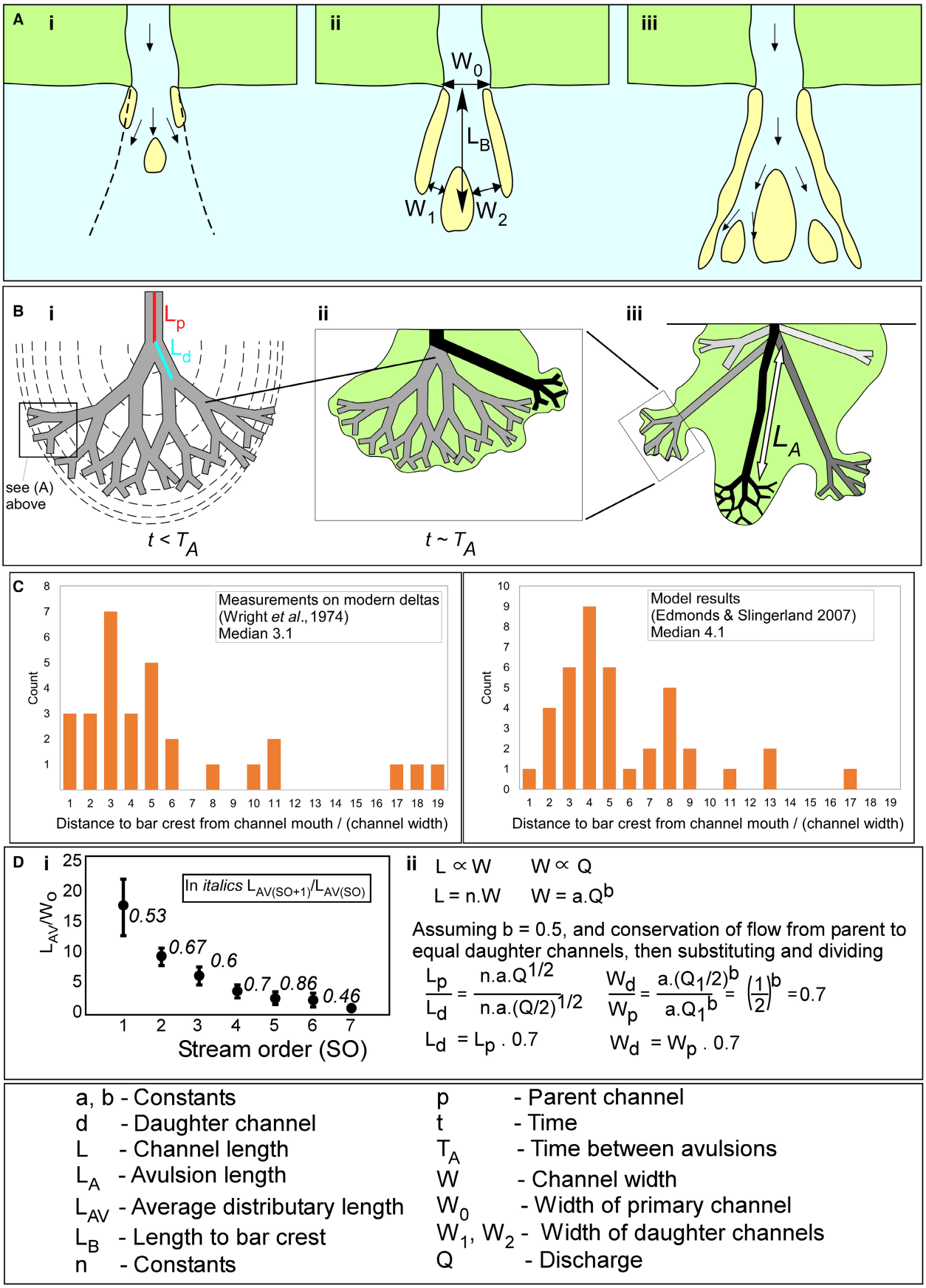

Fig. 1. The bifurcation-driven model for the development of channel patterns on fluvially-dominated deltas. (A) (i) A subaqueous triangular mouth bar and flanking subaqueous levées form at a river mouth; (ii) the levées extend, and the bar moves basinward, until the bar crest stabilizes at a distance L_B whereupon the extended channel splits to form two daughter channels of unequal widths, W_1 and W_2, and the process repeats; (iii) spawning progressively smaller channels and mouth bars (modified from Jerolmack, 2009). (B) As channel splitting proceeds, the system progrades, and a delta lobe develops. Avulsions can occur at any scale, but the longest (L_A) are expected to occur at the backwater length (Jerolmack, 2009) or at the delta head (Hartley *et al.*, 2017). (C) Modern deltas (Wright *et al.*, 1974) and modelling (Edmonds & Slingerland, 2007) suggest that mouth bars stabilize at a distance from the channel mouth that is three to four times the width of the channel which feeds them. (D) (i) Average non-dimensional distributary lengths against stream order for 11 deltas (from Edmonds & Slingerland, 2007). The numbers in italics show the ratio between the values for successive stream orders – which themselves have an average of 0.64. W_o is the width of the primary trunk distributary before it has split once. (ii) Assuming a constant relationship between channel width, W, and channel length, *L*, and that channel width is also related to discharge, *Q*, with b of the order of 0.39 to 0.5 (Mikhailov, 1970; Andrén, 1994; Edmonds & Slingerland, 2007), then, taking a value of 0.5 for *b*, and assuming that channels split discharge equally, a daughter stream segment [L_d, see B(i)] is expected to be seven tenths of the length of its parent channel (L_p), a result close to the measured values shown in (i). Similarly, daughter channels are expected to be around seven tenths of the width of a parent channel.

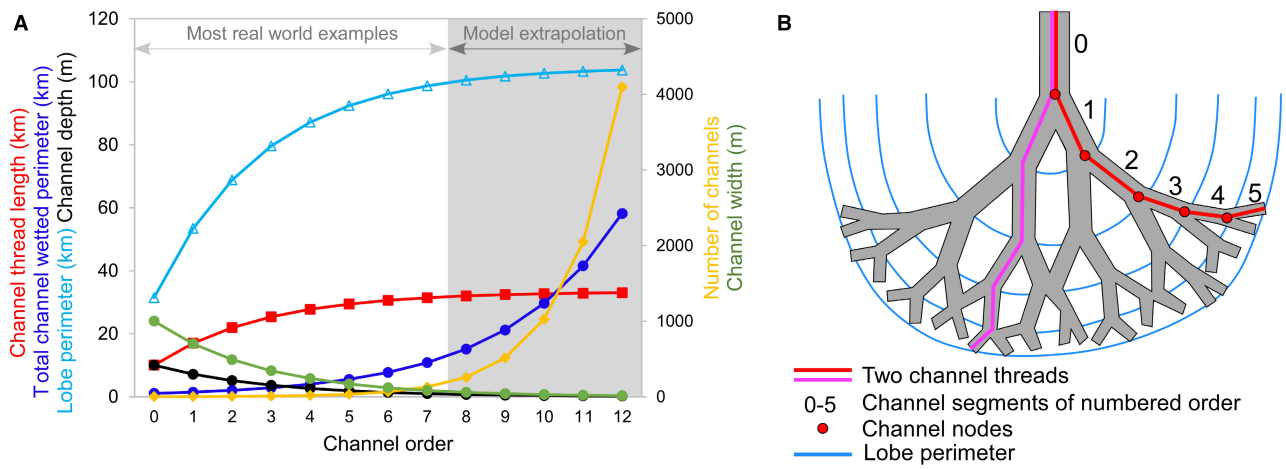

Fig. 2. The bifurcation-driven model predicts that at each bifurcation node, channels narrow, and channel segment length reduces. (A) After around ten bifurcations, new channel segments are so short that channel thread length, a close approximation of lobe width, barely increases. For progradation to continue the channel pattern must change. In this example, an initial (zero order) 1 km wide, 10 km long, 10 m deep channel has subsequent channel segments seven tenths the length of their parent channels. If channel width also decreases by seven tenths at each split, and cross-sectional area is preserved, then total channel wetted perimeter, an indication of bed friction, would have increased by a factor of 60 for 12th order channels, forming a system much less capable of transporting sediment. Few real-world examples display more than seven orders of channel split (Edmonds & Slingerland, 2007), and, in this example, by that point channel depths are less than 1 m. (B) Sketch based on Jerolmack & Swenson (2007) showing two channel threads, red and pink, and channel segment order numbers for the red thread.

short-lived, as a result of shallowing forced by deposition. By contrast, buoyancy dominated river mouths were considered to form a lunate mouth bar and straight, elongate, subaqueous levées that developed as result of a buoyancy-induced, weak, near-bed flow convergence that inhibits lateral spreading of coarser sediments, with the modern-day Mississippi River being the exemplar (Waldrop & Farmer, 1974; Wright & Coleman, 1974). Wright's work has been highly influential (Reading & Collinson, 1996). However, more recent studies (reviewed by Fagherazzi *et al.*, 2015), primarily using modelling approaches, suggest that many river-mouth deposits are better summarized in terms of two end member models: low inertia and high-inertia jets (Fig. 3).

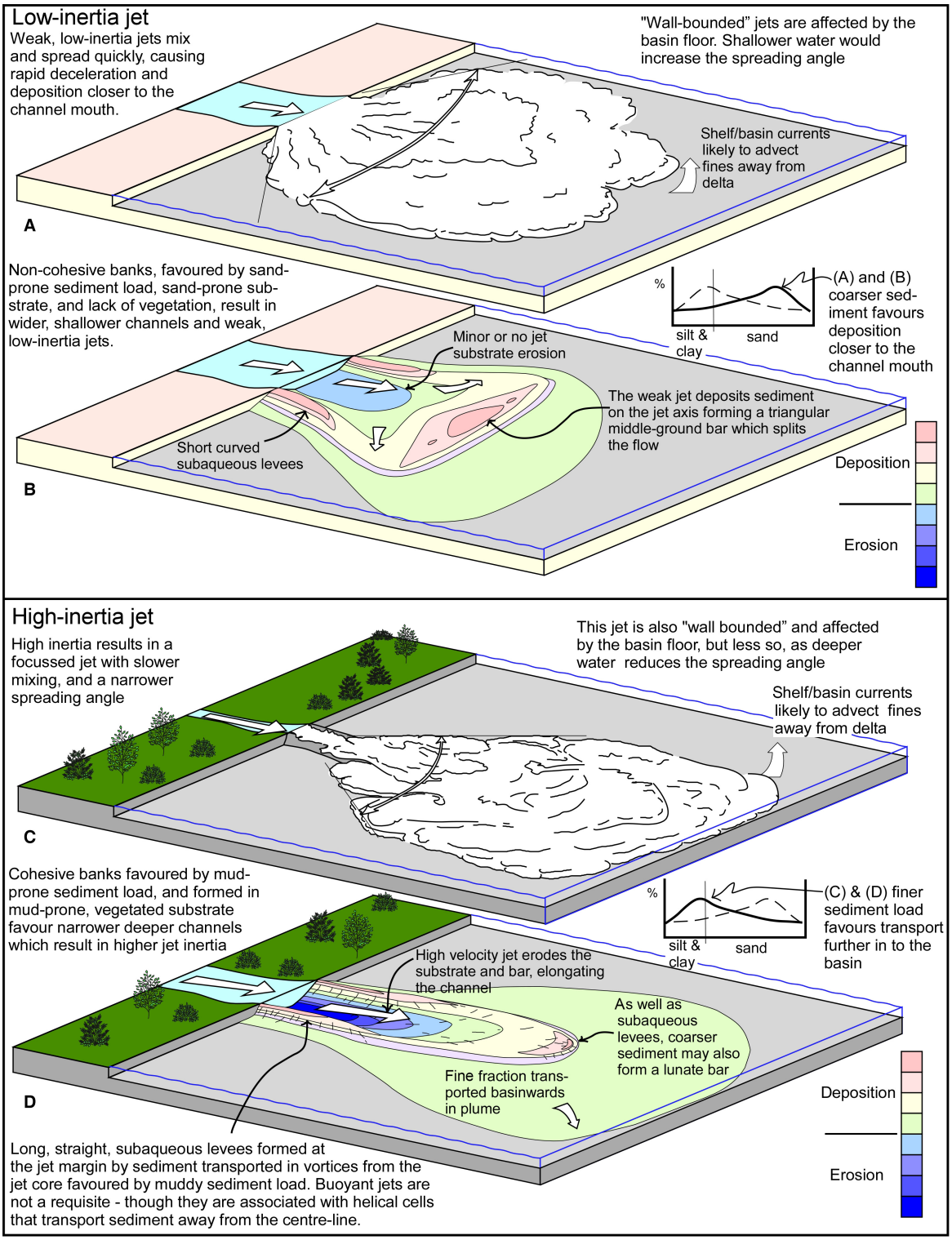

Fig. 3. Recent studies (Fagherazzi *et al.*, 2015) suggest that river-mouth deposits can be described in terms of two end member types of jet: low-inertia jets illustrated in (A) and (B); and high-inertia jets, shown in (C) and (D). Examples presented here support this division, but also extend the suite of associated deposits. Coloured depth contours based in part on Edmonds & Slingerland (2007).

Low-inertia jets are favoured by shallow, wide channels opening in to shallow water and by coarser grain sizes (Orton & Reading, 1993; Fig. 3A and B). Their deposits include the friction-dominated mouth bars of Wright (1977). Shallow, wide channels have higher ratios of wetted perimeter to cross-sectional area, and result in less focussed, lower-inertia jets that drop below critical transport velocities sooner, and deposit sediment closer to river mouths than high-inertia examples. Coarser grain sizes compound this (Axelsson, 1967). Shallow water forces the unconfined jet to expand laterally as a plane, bounded jet, and the shallower the water the stronger this effect. Interaction with the basin floor, through friction, and with the standing body of water via turbulent eddies, slows the jet and aids expansion. Expansion causes deceleration and deposition. Deposition occurs initially in marginal levées, and then on the jet centreline, where a small middle-ground mouth bar develops, grows and migrates basinward to stabilize three to four channel widths from the channel mouth (Wright *et al.*, 1974; Edmonds & Slingerland, 2007; Fig. 1C). The fully-formed bar splits the jet and the extended channel, and the process repeats.

High-inertia jets are favoured by deep, narrow channels that open in to deeper water and by finer grain sizes (Fig. 3C and D). High-inertia jets are characterized by long, straight, subaqueous levées formed at the jet margin by sediment transported in eddies from the jet core (Wright, 1977; Rowland *et al.*, 2010; Fagherazzi *et al.*, 2015). The well-developed levées focus the jet and maintain velocity along the jet centreline enabling substrate erosion, and transport of suspended sediment deep in to the basin. Though elongate subaqueous levées develop in granular material below experimental jets (Rowland, 2007; Rowland *et al.*, 2010), natural examples are favoured by: (i) muddy substrates (Geleynse *et al.*, 2011) and vegetation (Fagherazzi *et al.*, 2015), which result in cohesive river banks, and deeper, more flow-efficient channels with fixed positions (Rowland *et al.*, 2009); and (ii) a fine-grained, muddy, sediment load (Hoyal & Sheets, 2009; Kim *et al.*, 2009; Edmonds & Slingerland, 2010; Caldwell & Edmonds, 2014), which results in sediment transport in suspension beyond the river mouth (Falcini & Jerolmack, 2010). Nevertheless, resulting levées, mouth bars and channel fills are sand prone (Table 1). In contrast with Wright (1977), buoyant plumes are now considered an unlikely requisite for the formation of elongate subaqueous levées because: (i) a buoyant plume will not erode a mouth bar – a requisite for channel extension, and, for example, a key feature of the modern Mississippi River mouth (Fisk, 1961); (ii) many elongate subaqueous levées occur in lacustrine settings (Table 1) where buoyant plumes are less likely; and (iii) experiments show that buoyant plumes tend to form deposits on the jet centreline rather than elongate subaqueous levées (Rowland *et al.*, 2010). In addition to influencing the presence of stabilizing vegetation, climate, together with catchment area, may play a key role in delivering high peak discharges that favour high-inertia jets (Mulder *et al.*, 2003).

Pure jets are driven by momentum alone. Pure plumes are driven only by buoyancy, with intermediate flows described as forced plumes or buoyant jets (Crapper, 1977; Turner, 1979; List, 1982). Wellner *et al.* (2005) used the terms 'jet' and 'plume' more loosely, but perhaps helpfully, to describe axial and proximal sands as jet deposits, and distal and lateral mud-prone fringes as plume deposits. Buoyancy may be positive (hypopycnal flow), neutral (homopycnal flow) or negative (hyperpycnal flow; Bates, 1953). Positively-buoyant flows are more likely when warm, freshwater rivers with limited suspended sediment enter cold, saline water bodies (for example, the sea). By contrast, negative buoyancy is favoured when cold, turbid rivers enter warm, freshwater lakes (Mulder *et al.*, 2003).

METHODOLOGY

The approach adopted here has been to map the plan form, and plan form evolution, of depositional elements at fluvially-dominated river mouths. Some examples are based on historical maps, but many rely on interpretation of satellite imagery.

The satellite images were derived from Google Earth Pro and Google Earth Engine Timelapse which contain both high-quality, present-day imagery, with a resolution of around 1 m, and historical imagery, largely derived from Landsat data with a resolution of 30 m. Though most of the historical imagery is of lower resolution it benefits from being available for every year for the period 1984 to 2020, and is generally supplemented by a handful of additional high-resolution images for each delta over the same period. All of the studied imagery had been

processed to produce a 'true colour' image, i.e. a natural colour rendition, as would be seen by an observer at altitude. The images allow the scale of depositional elements to be measured, and associated metadata labels of rivers, lakes and infrastructure to be displayed. Such information has been supplemented by data from previous studies, including ground-based observations, allowing the documentation of typical water depths, grain size and depositional timescales (Table 1).

Furthermore, though satellite imagery on its own is the essence of remote sensing, its analysis is facilitated by established guidelines (Campbell & Wynne, 2011; Riebeek, 2013). For example, water is known to absorb light so that deep, clear water is typically blue or black. Shallow clear water may allow subaqueous forms to be studied. By contrast, high concentrations of suspended sediment typically turn water light brown in colour, and at certain angles light is reflected from water surfaces rendering them white or light grey. Additionally, surface wind waves are commonly resolved on high resolution images, and can be helpful in distinguishing water from bare sediment surfaces. Bare sands are generally white in colour, and muds are commonly various shades of brown, but each will vary depending on their provenance. Different plants are seen in diverse shades of green, with many transitioning to shades of brown in autumn and winter. Vegetation can also be expected to change sensitively with respect to elevation above the water table, being different, for example, on elevated levées and in semi-permanent lakes. Topographic analysis can be extended by mapping the shoreline, and pond and lake margins, as well as strandlines, each of which act as elevation contour lines. Topography is further revealed by noting how waves refract around subaqueous delta front irregularities, by recording shadows cast by steep slopes and tall vegetation, and also by observing brightly lit regions that may record steep slopes or vegetation that face the sun. The temporal evolution of deposition can be picked out by a succession of plants developing as bare sediment is colonized, and also by cross-cutting relationships, as produced by an avulsed channel, or in wave-dominated deltas by wave ravinement surfaces (Ainsworth *et al.*, 2019). In general, here, it has largely been revealed by historical satellite imagery.

With these guidelines to interpreting satellite imagery at hand, together with metadata for river courses, and maps from previous studies available as image overlays, the approach has been to digitize depositional element outlines for a series of timesteps for each example. The outlines variably reflect a wide range of features that may indicate an element margin, the shoreline, a change in elevation picked out by vegetation, a shadow, or a brightly-lit slope. Detailed images associated with some of the examples presented below illustrate the process.

EXAMPLES OF CHANNEL-MOUTH DIVERSITY ON MODERN FLUVIALLY-DOMINATED DELTAS

In the six examples which follow, analysis of satellite imagery and review of previous studies reveals a broad suite of river-mouth deposits which change laterally across individual delta lobes, between lobes, and along the length of elongating distributaries, even though the ranges of grain size (coarse silt to fine sand) and water depth (2 m to over 25 m) are limited (Table 1).

The Volga River Delta sub-lobe, Caspian Sea, Russia: a lobate delta

An active, likely very shallow water [<2 to 3 m (Overeem *et al.*, 2003)], sub-lobe of the Volga Delta (Fig. 4A) is characterized by mouth bars with a range of plan-form geometries – tongues, fronds and splays. Prior to their detailed description below, Fig. 4B offers an opportunity to illustrate an application of the methodology for interpreting satellite imagery outlined above, and in particular to point to how distinct depositional elements, their margins and relative timing, can be identified.

Features aiding satellite image interpretation

On each of the detailed images shown in Fig. 4B, numbers, (1) to (15), locate key features. White areas are interpreted as subaerial sand (1) deposited at a higher stand of lake level, with strand lines (2) recording lake-level fall. Consistent with the known very fine grain size of the Volga Delta (Table 1), even at the highest image resolution there is no indication of dune-scale bedforms on the exposed sand platforms. Water colour (3), (4), (5) and (6) varies across the images. Dark green regions (3) are interpreted as deeper (only a few metres) clear water. Bright green areas (4) onlap, and become darker away from subaerial sand transitioning in to the dark

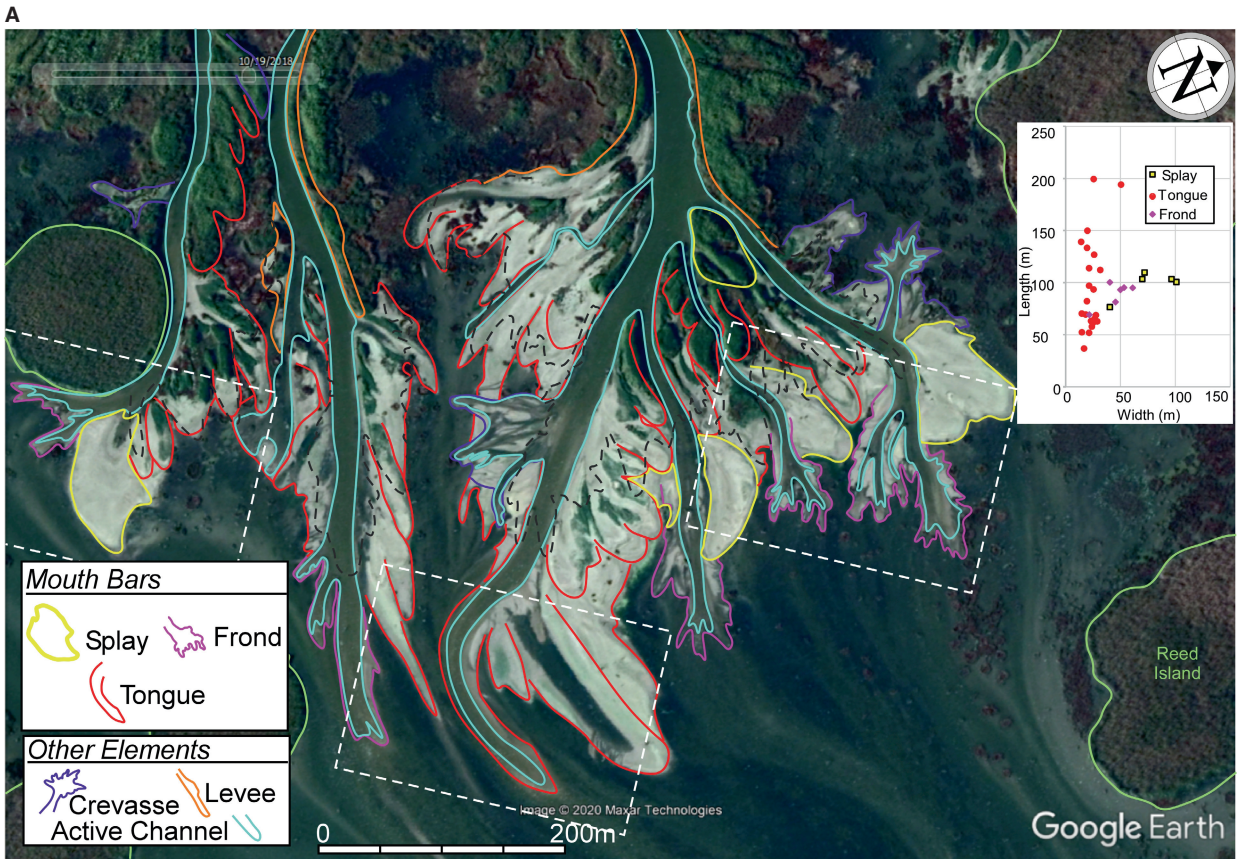

Fig. 4. (A) Overview of terminal channel systems and river-mouth deposits on a minor lobe of the Volga Delta, Russia. The river-mouth deposits are characterized by a range of mouth-bar forms, described here as splay, frond and tongue-shaped mouth bars. Each form appears to display a distinctive width–length ratio, with more elongate forms hypothesized to be have been formed by increasingly inertia-dominated flows. Splay-shaped mouth bars are relatively equant sandbodies which either divert channels, or are bisected by them, and are interpreted as friction-dominated. By contrast, elongate tongues of sand are interpreted as inertia-dominated mouth bars, and frond-shaped mouth bars are considered to record intermediate flows. Channels record the elongation of dominant threads. Image from October 2018. Black dashed line shows the shoreline position two years previously, in September 2016. Note that, despite the progressive growth of vegetation, comparable scales and morphologies allow older river-mouth deposits to be recognized and their origin inferred. Image located at 45°41′7.99″N 48°11′44.32″E and on Fig. 14A. White dashed rectangles locate detailed images shown on (B). Satellite image from Google Earth, Image © 2020 Maxar Technologies, Image Landsat/Copernicus.

green of deeper water (Fig. 4Bi). These bright green regions are located away from active channels, reveal something of the lake floor, and are interpreted as shallow, clear water, with the green colour considered to indicate the presence of green algae in the water column. The central, presumably deeper portions, of active channels are green–olive (5) in colour, and transition at their margins, and mouth bar termini, to light brown (6). The transition in colour is interpreted to record a gradual shallowing of water depth, and increased visibility of subaqueous sand in shallower water. By contrast, bar fronts and margins are characterized by a sharp colour change to dark green, interpreted to reflect a relatively steep slope in to deeper water. Shadows cast towards the north (7) give an indication of topography at channel margins, and also of vegetation height. Three forms of vegetation are recognized. Circular islands (8) cast clear shadows and form in the lake, but are incorporated in to the delta plain as progradation proceeds, and are interpreted as reed islands (Richards, 2018). Bright green regions on sand flats that cast no clear shadows are considered to record low-lying vegetation (9) that is succeeded by taller

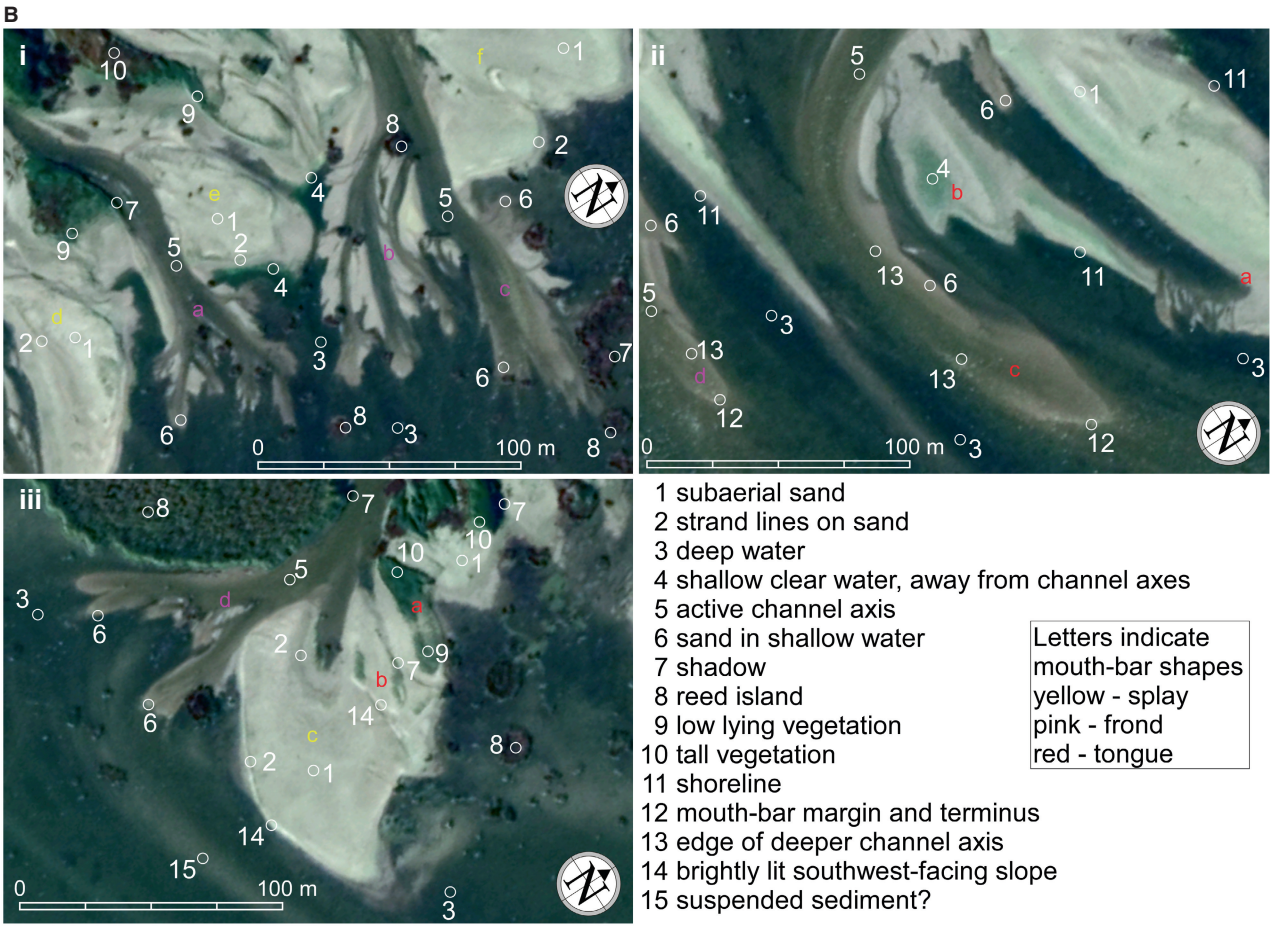

Fig. 4 (Continued). (B) White, 5 m diameter circles, and numbers 1 to 15, locate key features of river-mouth deposits on the Volga Delta. The highlighted features support the interpretation, and are discussed in detail in the text. The same depositional elements are outlined on (A) (which also locates these images) but, for clarity, are shown here uninterpreted: (i) three partially subaqueous frond-shaped mouth bars, a to c, that dissect earlier, subaerial, stranded splay-shaped mouth bars, d to f; (ii) tongue-shaped mouth bars, and (iii) a splay-shaped mouth bar c, with prior tongue-shaped mouth bars, a and b, and a later frond-shaped mouth bar, d. Satellite images from Google Earth, Image © 2020 Maxar Technologies, Image Landsat/Copernicus.

vegetation (10) over time (Fig. 4Bi). Shorelines (11) are locally crisply defined, as at the junction of white sand (1) and dark-green, deeper water (3), and have in several instances have been taken as indicative of mouth bar margins (Fig. 4Bii). In other cases, active, subaqueous, mouth-bar margins were mapped at an abrupt change (12) from shallow sand (6) to deep water (3) (Fig. 4Bii). Figure 4A captures the margins of both abandoned and stranded, and recently-active, subaqueous mouth bars as red lines. Active channel segments are highlighted as cyan lines on Fig. 4A – their margins are clear where channel banks are vegetated, but indicative across subaqueous mouth bars where flow is no longer fully confined (13) (Fig. 4Bii). In some examples, relative timing of depositional elements is indicated by historical satellite data, as in the Fig. 4Biii area where an image from 2016 shows a jet at the location of (and at the scale of) mouth bar b, but suggests deeper water at the positions of mouth bars c and d. Relative timing is also indicated by vegetation which picks out mouth bar a, and by doing so suggests that it pre-dates the largely unvegetated mouth bar, b (Fig. 4Biii). In a similar way, mouth bar c is subaerial, with an edge marked by strandlines (2), and a brightly lit south facing slope (14), and is considered to have been deposited at a higher lake level than mouth bar d which is subaqueous, connected to the active channel, and considered to be the last formed mouth bar (Fig. 4ABiii).

Elongate, curved regions of lighter colour in the offshore (15) may indicate suspended sediment, though the local active channel (5) appears to run with clear water (Fig. 4Aiii).

Distinct mouth bar styles

At their tip, tongue-shaped mouth bars display a lunate terminal bar with a gradual stoss and a steeper lee side (Fig. 4ABii). The bar links seamlessly to paired, elongate, marginal levées which curve away from the axis of the parent channel (Fig. 4A). Successive bars are abandoned at lengths of 200 m or less, with a new tongue-shaped mouth bar forming following a bar–levée breach, and older more proximal bars becoming increasingly vegetated (Fig. 4A). Though experimental jets have yet to produce directly analogous forms, they have produced similar features – axial channel erosion, elongate sand-prone levées (Rowland *et al.*, 2010) and curved terminal bars (Wellner *et al.*, 2005; Lang *et al.*, 2019). Numerical simulations by Edmonds & Slingerland (2007) also produced somewhat similar forms, differing in displaying straight levées, less elongate sediment bodies, and in being a transitional state prior to the development of stable middle-ground mouth bars. No such transitions are seen in this example. Following Wright (1977), and cognisant of the experimental results, the tongue-shaped mouth bars are interpreted as the product of high-inertia river-mouth jets.

Frond-shaped mouth bars are characterized by channel splitting, and by an irregular outline (Fig. 4Bi). Detailed review of satellite imagery suggests that channel splitting reflects, at least in part, the development of diminutive frond and middle-ground mouth bars. As with tongue-shaped mouth bars, water depth variations indicate that gradual stoss and steep lee-side terminations predominate, and as a result the areas between frond fingers are hypothesized to be relatively sand poor. Unlike tongue-shaped mouth bars, simulations and experiments are not known to have mimicked frond-shaped mouth bars.

Splay-shaped mouth-bars are characterized by a sand sheet with a steep front, and by a short, tongue-like feeder channel. They bear a resemblance to experimental deposits formed by radial flow expansion (Shaw *et al.*, 2018) and bedload transport (Daniller-Varghese *et al.*, 2020). Parent channels appear to lengthen by either cutting through, or diverting around, the splay Fig. 4A.

The three mouth-bar styles, tongue, frond and splay, have median length–width ratios of 3.7, 1.8 and 1.5, respectively. More elongate forms are interpreted to reflect higher-inertia jets. Serial satellite images show that two to six depositional elements develop at the end of each distributary channel over a period of two years. Fidolini & Ghinassi (2016) described features from the rock record similar to tongue and splay-shaped mouth bars, and considered that they formed at different stages of river flood. Following that approach, it is hypothesized that levée breach, river-axis erosion and channel elongation via progradation of tongue and frond mouth bars occurs at, or close to, the flood peak, whereas at lower stage, or during smaller floods, when water depth is reduced and discharge is lower, and bedload transport more important, those bars form a barrier to flow, and friction-dominated splay-shaped mouth bars develop. Since different river-mouth deposit styles occur concurrently, long-term changes in base level, sediment calibre or climate may not be required to produce a range of river-mouth deposits. The images in Fig. 4 lack ground truth data. However, channels and levées in the adjacent Astrakhan nature reserve (Overeem *et al.*, 2003) suggest a limited grain-size range, tightly distributed around 90 μm, for both channels and levées.

The Red River Delta in Lake Texoma, Texas, USA: an elongate delta

The Red River Delta partially fills a 2 to 3 km wide valley at the western edge of the Lake Texoma reservoir (Fig. 5). Satellite image interpretation allows sand-prone, river-mouth deposits to be inferred (Olariu *et al.*, 2012; Fig. 5), and shallow cores through river-mouth sediments dating from *ca* 1995 to 2016 confirm their presence (Howe, 2017). Previous studies suggest: (i) a two-phase evolution, with lobate morphologies and multiple channels transitioning to an elongate delta and a single dominant thread in 1981 (Olariu *et al.*, 2012); and (ii) a late channel with 'blow-out' overbank wings formed without sand reaching the river mouth (Tomanka, 2013; Huling & Holbrook, 2016; Howe, 2017). The extension of the Red River as a dominant, elongate channel thread is clear (Fig. 5). However, river-mouth deposits have been highly variable, frond-like in 1952, but characterized by a fan shape in 1976, with intervening fan and frond outlines (Fig. 5A). Middle-ground mouth bars dominated from 1984 to 1986 (Fig. 5A) followed by an elongate, levéed channel with a subordinate marginal system that was fan-shaped in 1993 and in recent times, with intervening

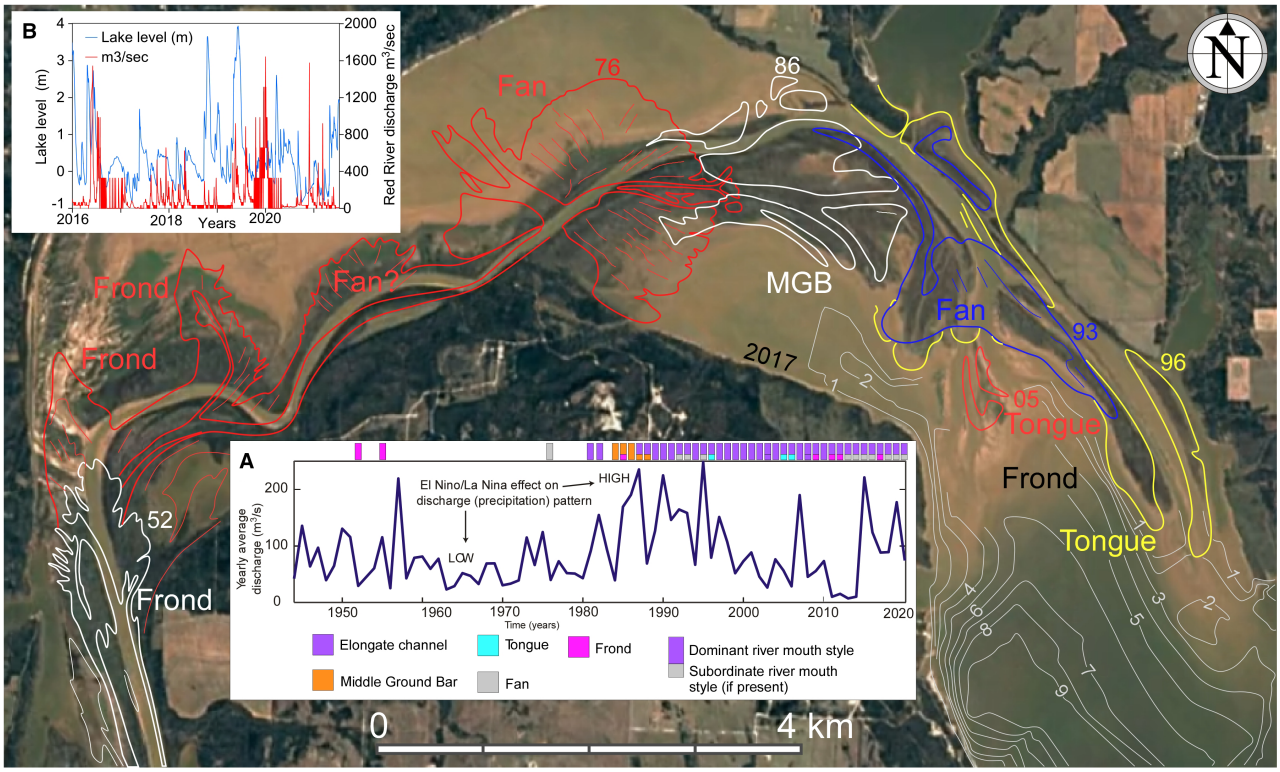

Fig. 5. In the last 50 years the Red River has extended by 15 km as a single elongate thread in to the Lake Texoma Reservoir, Texas, USA. Over that time a range of river-mouth styles developed. Sparse satellite images (from 1952, 1954 and 1976; Olariu *et al.*, 2012) suggest an early history of frond-shaped mouth bars, sections of simple levéed channel, and fan-shaped sediment bodies, described here as 'river mouth fans'. As recorded by the bar chart, annual images from 1984 onward (Google Earth©) reveal triangular middle-ground mouth bars (MGB) from 1984 to 1986 and a dominant, elongate, levéed channel thereafter, with subordinate tongue and frond mouth bars and river-mouth fans. It is difficult to relate this variability to (A) annual discharge, which fluctuates with the El Niño/La Niña effect (modified from Olariu *et al.*, 2012), or to (B) more limited records of lake-level oscillations. Discharge and lake level data from USGS (https://waterdata.usgs.gov/nwis). The satellite image dates from 2017. In white, isobaths in metres date from 2002, and are modified from Olariu *et al.* (2012). The satellite image dates from 2017, is from Google Earth Engine Timelapse and located at 33°56′40.20″N 96°54′5.23″W.

tongue (2005) and frond-like mouth bars (2017). Water depths are shallow, less than 10 m originally (Olariu *et al.*, 2012), shoaling to 1 to 5 m as river-mouth deposits develop (Fig. 5). Flows are likely to have been hyperpycnal (Olariu *et al.*, 2012), and river-mouth sands are medium to very fine-grained (Howe, 2017). Decadal variations in discharge, linked to the La Niña – El Niño effect, resulted in higher discharges in the 1980s and 1990s (Olariu *et al.*, 2012). However, as addressed in discussion below, it is difficult to link such decadal fluctuations to evolving river mouth geometries (Fig. 5A), or to determine the influence of oscillating lake-levels (Fig. 5B). Regardless, the example shows that a single system over a restricted time period can display a wide range of river-mouth deposit styles.

The Catatumbo River Delta, Lake Maracaibo, Venezuela: an elongate delta

The Catatumbo River Delta in Lake Maracaibo displays elongate, straight distributary channels (Fig. 6A). The geometry is interpreted to reflect high-inertia jets, favoured by relatively deep water, vegetated levées, a muddy substrate and a mud-prone sediment load, with a relatively fine-grained sand fraction (fine lower to coarse silt; Hyne *et al.*, 1979). However, this river mouth style did not occur in isolation. On the southern distributary, subaerial, vegetated, middle-ground mouth bars (colour filled on Fig. 6A and shown in detail on Fig. 6B) developed in 1984 to 1989, and 1992 to 1999, causing the distributary channel to split. Each time, the split was unequal, and

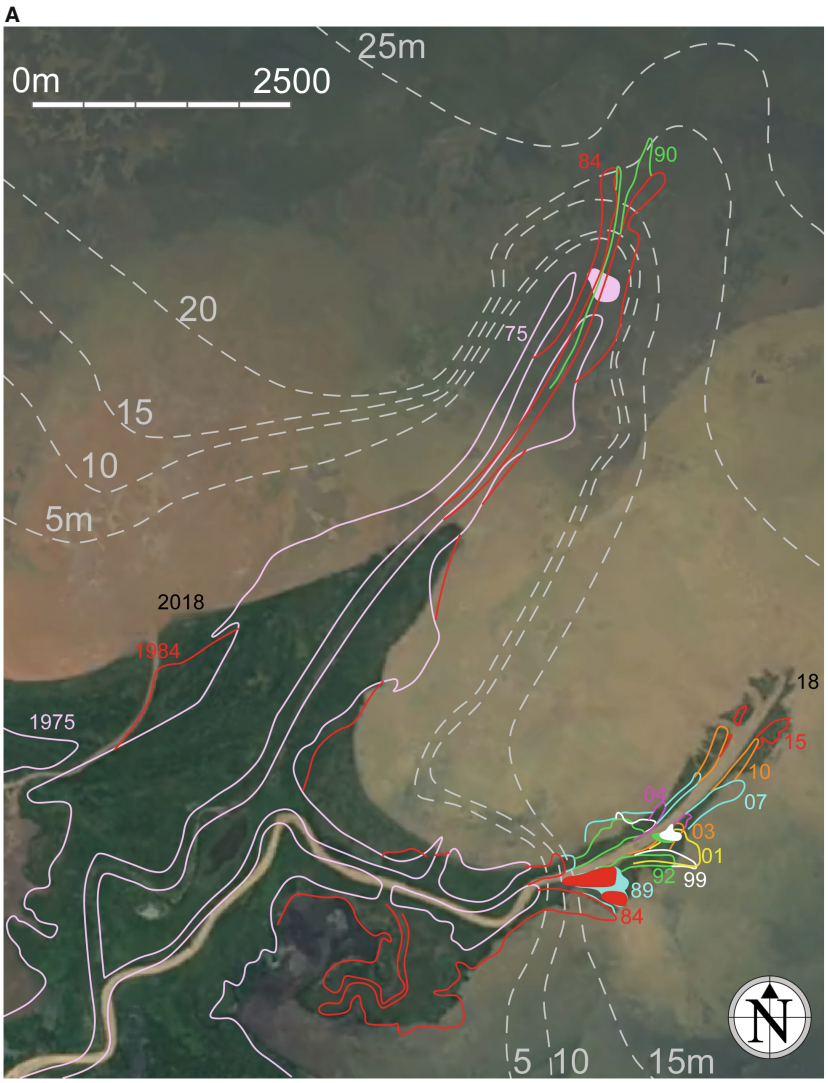

Fig. 6. (A) The Catatumbo River Delta, Lake Maracaibo, Venezuela, is characterized by straight, elongate distributaries, but also by rare, vegetated, middle-ground mouth bars. Coloured lines capture shoreline positions from 1975 to 2015. The mouth bars are colour filled, and occur from 1984 to 1989, and from 1992 to 1999 on the southern distributary and in 1975 on the northern distributary. The 1975 shoreline and the dashed isobaths are from Hyne *et al.* (1979). Later shorelines are based on Google Earth time-lapse imagery (B) which shows the mouth bars rotating clockwise and the southern distributary channel elongating along the dominant channel split. The satellite image dates from 2018 and is from Google Earth, Image Landsat/Copernicus. Image located at 9°20′17.86″N 71°46′10.16″W.

a dominant northern split persisted, whereas southern branches were abandoned, and intervening progradation was dominated by channel elongation. Prior to abandonment in 1991, the northern branch displayed a similar evolution with a middle-ground mouth bar developing in 1975 (Hyne *et al.*, 1979), but channel elongation occuring from 1984 to 1991. Two main sandbody types are recognized, 'bar-finger' mouth-bar sands perpendicular to the shoreline, and transgressive beaches parallel with the shoreline (Hyne *et al.*, 1979), but middle-ground mouth bars (and crevasee splays Fig. 5B) are also likely to be preserved as a minor component. The Raccourci Old River, Lower Mississippi River, a type example of a tie channel (Rowland *et al.*, 2009; a type of elongate, jet formed channel; Table 1), developed a similar middle-ground mouth bar from 2003 to 2005.

The lacustrine Omo River Delta, Kenya and Ethiopia: an elongate delta

After 2001, the three main distributary channels on the Omo Delta developed the same three-fold progression of distinct river-mouth deposits (Fig. 7A). From 2002 to 2004, during lake-level fall, fan-shaped deposits developed, each characterized initially by weakly-defined, shallow, radiating channels, and then, following flow capture, by a central, larger, well-defined channel that cut across the fan to feed the next river-mouth deposit. Satellite images of the Omo, and of similar features in Sarygamysh Lake, Turkmenistan (Table 1), suggest that the fan-shaped deposits developed subaqueously rather than as subaerial terminal fans. From 2005 to 2007 delta lobes

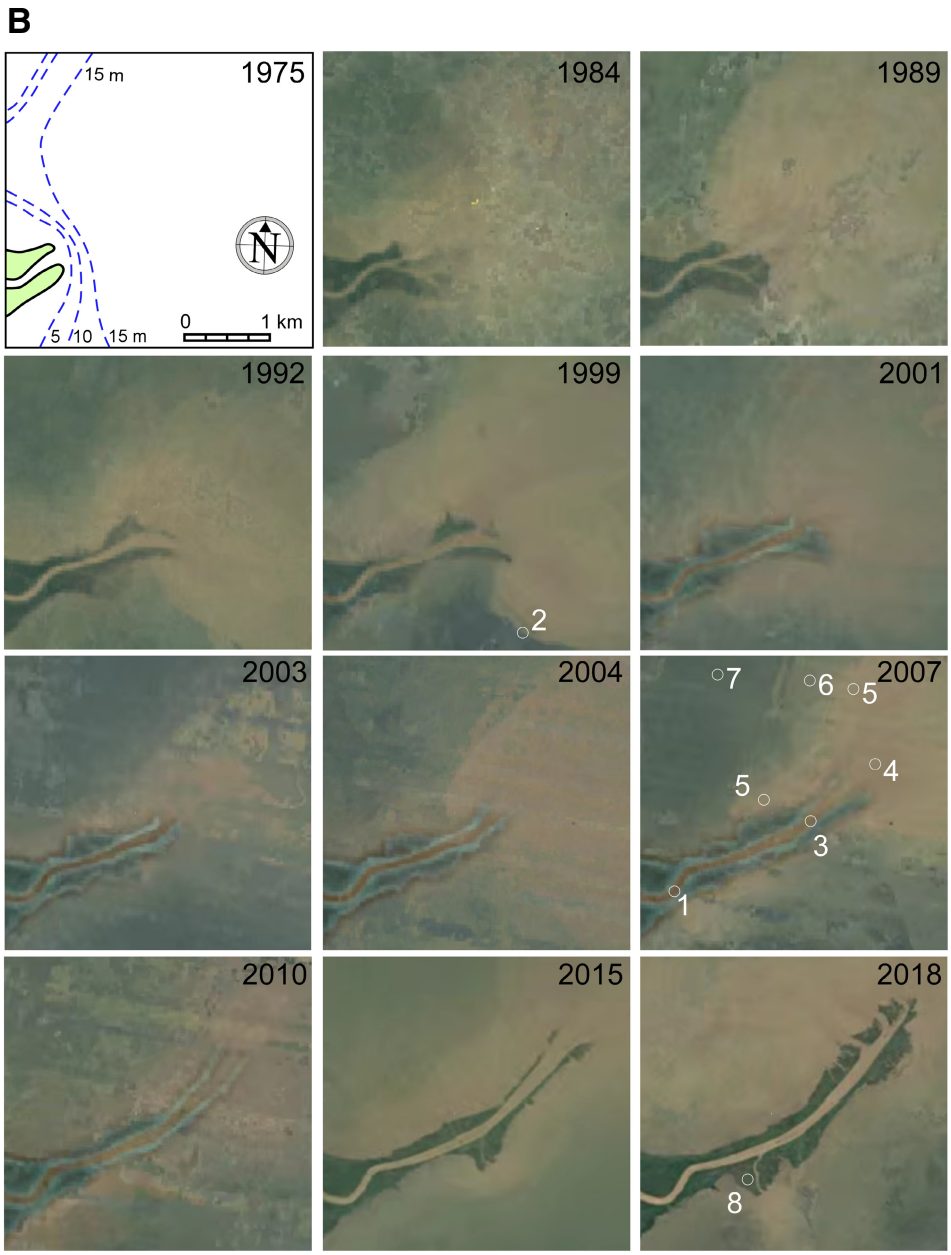

Fig. 6 (Continued). (B) The 12 timesteps shown here present data used to capture the evolution of the southern mouth of the Catatumbo River in Lake Maracaibo Venezuela on (A). The map, from Hyne *et al.* (1979), is shown at the same scale and orientation as the satellite images, with the green ornament outlining levées at the river mouth in 1975. Blue dashed lines are isobaths. The images are true colour representations from Google Earth Engine. Colour variations reveal changes in image processing and/or acquisition, with images from 1984 to 1999, 2001 to 2010 and 2015 to 2018 appearing as colour-consistent, but contrasting, sets. Despite this variability, all of the images show the river as a sinuous brown ribbon (1; 2007). The brown colour extends away from the river mouth, and is interpreted to record a plume of suspended sediment. The size of the plume varies, for example it was small in 2003, but larger in 2004. At times, the plume margin is relatively sharp (2; 1999). More commonly the brown colour at the river mouth fades slowly (3–4–5–6–7; 2007), via lighter browns to green hues interpreted to record deeper water with lower concentrations of suspended sediment. The darkest green colours are interpreted as vegetated channel levées and mouth bars. The latter are well-developed in 1984 and 1989, and also recognized in 1999, but they do not result in long-lived channel bifurcations. Instead, they rotate away from a dominant northern channel segment, become part of the southern levée and the channel extends without permanent bifurcation. Though smaller in extent, the channel is also fringed by suspended sediment that attests to overbank flow, and crevasse deltas (8; 2018).

developed, characterized by middle-ground mouth bars and channel splitting (Fig. 7B), and were followed by channel elongation during overall lake-level rise. The possibility of base-level being a control on river mouth deposit style is addressed in discussion below. The system is relatively fine-grained, with river-margin deposits ranging from 60 to 200 μm (Butzer, 1970).

The Cubit's Gap Crevasse Delta, Mississippi, USA: a lobate delta

Following a man-made cut in 1862 the Cubit's Gap Crevasse Delta developed naturally (Holle, 1951; Welder, 1955; Alexander *et al.*, 2012). Rather than developing marginal levées and a single large mouth bar (Fig. 3), the flow spread concentrically, and deposited a shoal only a few hundred feet from the gap (Welder, 1955; Fig. 8). As the shoal grew, it became an obstruction to flow, and by 1870 the current was forced to dissect it with a spray of wide, shallow channels, three of which persist to the present day. The northern portion of the delta is characterized by a single channel, the 'Main Pass'. Anomalous depth and width, and a large subaqueous bulge at its terminus in 1877 suggest that it was the dominant distributary. Up until 1903 the Main Pass was straight, and though associated with several minor branches towards the north, there is no indication that the channel had split to form two equivalent, deep, daughter channels, nor that it had deviated around a mouth bar until sometime after 1922. Like the Southwest Pass of the Mississippi Bird Foot Delta (Fisk, 1961), rather than repeatedly splitting, the channel extended over time by cutting straight through river-mouth deposits. By contrast, the south-east portion of the delta displays a more conventional branching pattern, though long, straight channel reaches developed there too, most notably Octaves Pass, which also initiated on the 1870 subaqueous platform, but by 1877 existed as the dominant channel in a distributive pattern. In later maps the small distributaries disappear, Octaves Pass appears as a single long channel segment, and its early history of progressive straight growth can no longer be discerned (see Welder, 1955).

The Atchafalaya Delta, Mississippi, USA: a lobate delta

The basic form of the Atchafalaya Delta was established in just two or three years, and particularly during a major flood in 1973 (Van Heerden & Roberts, 1988; Fig. 9). Much of the rapid growth was in the form of subaqueous and subaerial levées to channels at mouth bar margins. Once vegetated, the levées define islands, transforming mound-shaped subaqueous mouth bars to display a 'crab-claw' geometry characteristic of many friction-dominated delta lobes (Belevich, 1956; Axelsson, 1967; Wellner *et al.*, 2005) with central lows marked by finer-grained sediments and algal mats (Van Heerden & Roberts, 1988). Although new bars and islands develop over time, rather than simply growing in sequence, all of the islands and bars continued to accrete over time, with upstream growth almost as important as downstream growth.

Summary of river mouth-deposits

Most of the six examples lack extensive ground truth data, and they are unlikely to have documented the full range of river-mouth deposits. There is no guarantee that forms which are similar on satellite imagery will be comparable in detail, for example in terms of formative flows, grain size or ornamenting bedform styles. Nevertheless, a preliminary summary of the different forms can be attempted (Fig. 10), if only to stimulate critical review, and further study. The following observations are suggested.

1 River-mouth deposits display more diversity than is commonly recognized, beyond the friction, inertia and buoyancy-driven mouth bars described by Wright (1977), and the two styles of high-inertia and low-inertia jet deposits described above (Fig. 3). This is particularly true for ancient successions and modern deltas which have generally been described in terms of single river-mouth deposit styles.

2 Not all river-mouth deposits can be described as mouth bars, a term which is most usefully employed to describe a shallow-water bar at the mouth of a river, and excludes levées, channels and river-mouth fans.

3 Distinct channel-mouth deposits can alternate along a single prograding channel thread, and may exist as coeval lateral equivalents at multi-threaded delta fronts. These observations are at odds with a fractal, self-similar model for delta lobes, and suggest that some elongate channels have a complex origin.

4 Fan-shaped river-mouth deposits (as seen, for example, on the Omo Delta, Fig. 7) are geometrically similar to alluvial fans and subaerial terminal fans, but differ in that they appear to

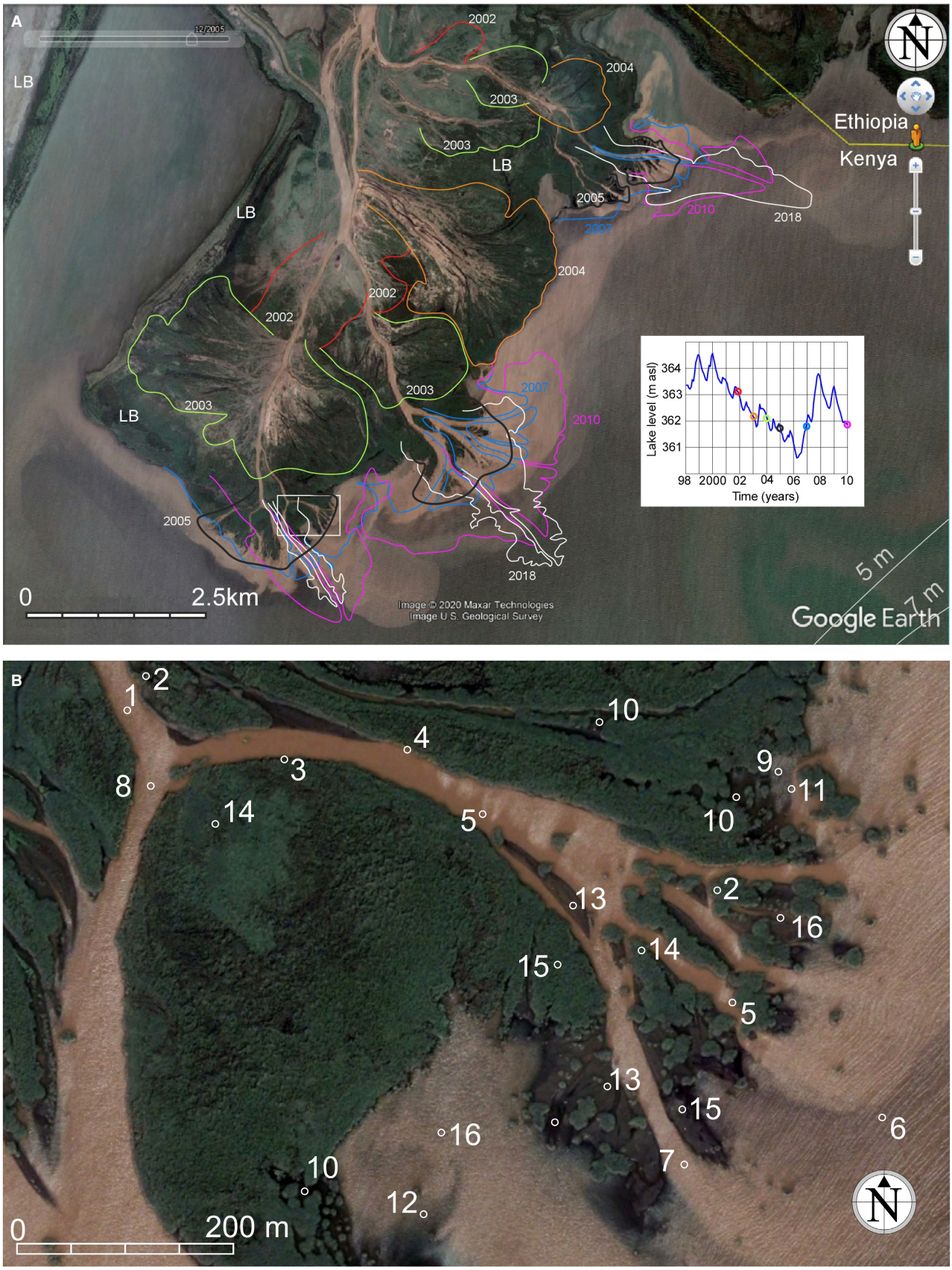

Fig. 7. (A) The lacustrine Omo Delta in Kenya (and, partially, Ethiopia, top right). River-mouth deposit style appears to vary as lake-level changes, with river mouth fans being replaced first by lobes with middle-ground mouth bars, and then by elongate channels. Lines show simplified delta-front shoreline positions from 2002 to 2018 based on Google Earth imagery. LB denotes areas of exposed lake bed. The image shown dates from December 2005 and is sourced from Google Earth, Image © 2020 Maxar Technologies, Image U.S. Geological Survey. Lake-level curve from Velpuri *et al.* (2012), and water depths from Carr (2017). Satellite images suggest that lake level rose from 2010 to 2018. Image located at 4°26′38.51″N 35°59′13.39″E. The white rectangle on the southernmost lobe locates (B). (B) Detail showing a period of middle-ground mouth bar development and channel splitting at the southern mouth of the Omo River in 2005. The image shows a portion of (A), and is from Google Earth, Image © 2020 Maxar Technologies, Image U.S. Geological Survey. The brown colour of the active parent channel (1) is interpreted to record suspended sediment, and is confined by green vegetation (2). Shadows at southern channel edges (3), and more brightly lit northern margins (4) suggest that the vegetation and/or channel banks are of some height. Surface waves confirm the presence of water. Light streaks, oriented SSW–NNE, that develop in the northern half of north-west/south-east trending channels are interpreted as surface riffles (5) generated by wind blowing from the SSW beyond the lee of vegetated islands. Open-lake waves 1.2 km south of the image have crests that trend WSW–ENE, but refract as they approach the delta front and become sub-parallel to the shoreline (6). Such waves lose their form as they enter distributary channels (7), which may display local wind waves with crests trending WNW–ESE if the channels are long enough and suitably oriented (8). Not all of the water is brown in colour. Surface riffles also develop on dark brown-black regions (9) which are interpreted as water with low or no suspended sediment (10), and occur away from active channels and in delta plain ponds. Sharp (11) and transitional boundaries (12) between these two water types occur and are interpreted as the margins of sediment laden plumes. Dark brown regions that lack either surface wave or vegetation are interpreted as subaerial sand (13). The parent channel is interpreted to split around the heads of two orders of middle ground bars, both of which display a characteristic crab-claw subaerial topography (Van Heerden & Roberts, 1988), with an elevated bar head (14) and margins (15; channel levées) and a central low (16). The larger upstream bar is more vegetated and interpreted to have formed first. Downstream a spray of smaller bars split the flow in to four smaller channels. The larger bar may have had a similar origin, but there is no clear record of it on the image.

form subaqueously and scale with, and are equivalent to, other river-mouth deposits, such as river-mouth bars and elongate channels.

5 Aspect ratio is hypothesized to be a useful indicator of the degree of inertia of formative jets. Elongate river-mouth deposits are interpreted to have been formed by higher-inertia jets, whereas more equant forms are likely to be the product of lower-inertia jets. Fan-shaped deposits are interpreted to have been formed in very shallow water by jets experiencing high friction. These interpretations allow different river-mouth deposits to be arranged along a spectrum from low-inertia fans, to high-inertia elongate channels with well-developed subaqueous levées. The spectrum can be divided in to two by whether or not a mouth bar develops that the jet is unable to erode and which splits, diverts or spreads the flow as a result.

6 Wellner *et al.* (2005) interpreted the coarse, axial, proximal component of jet deposits (mouth bars) at the Wax Lake Delta to record the back-fill of jet-scour pools formed at peak flow (orange ornament on Fig. 10C). However, unlike examples from the Volga Delta, scour pools are absent from satellite images of both the Wax Lake Delta and the adjacent Atchafalaya Delta, suggesting that, if they do occur, they are always quickly filled, probably as the flows which formed them wane.

7 Most flume experiments, simulations and many models of river-mouth deposits, consider the development of a single mouth bar, from a single channel mouth. From them, it would be possible to develop the view that mouth bars form progressively, and that once a mouth bar is formed, deposition shifts to the development of new mouth bars at the end of each new distributary channel split. Modern examples suggest more integrated growth patterns. Crevasse deltas initiate as shallow, sand-prone shoals rather than large mouth bars (Fig. 8; Van Heerden & Roberts, 1988), and although new bars and islands develop over time, rather than growing only as a sequence of offlapping forms, all of the islands and bars continue to accrete over time, with upstream growth almost as important as downstream growth (Fig. 9; Van Heerden & Roberts, 1988; Wellner *et al.*, 2005).

8 As channels split, the distributary network covers an increasingly large portion of the delta lobe, so that new channels eventually interfere and some coalesce. This effect is not considered on Fig. 2 but may be important in creating

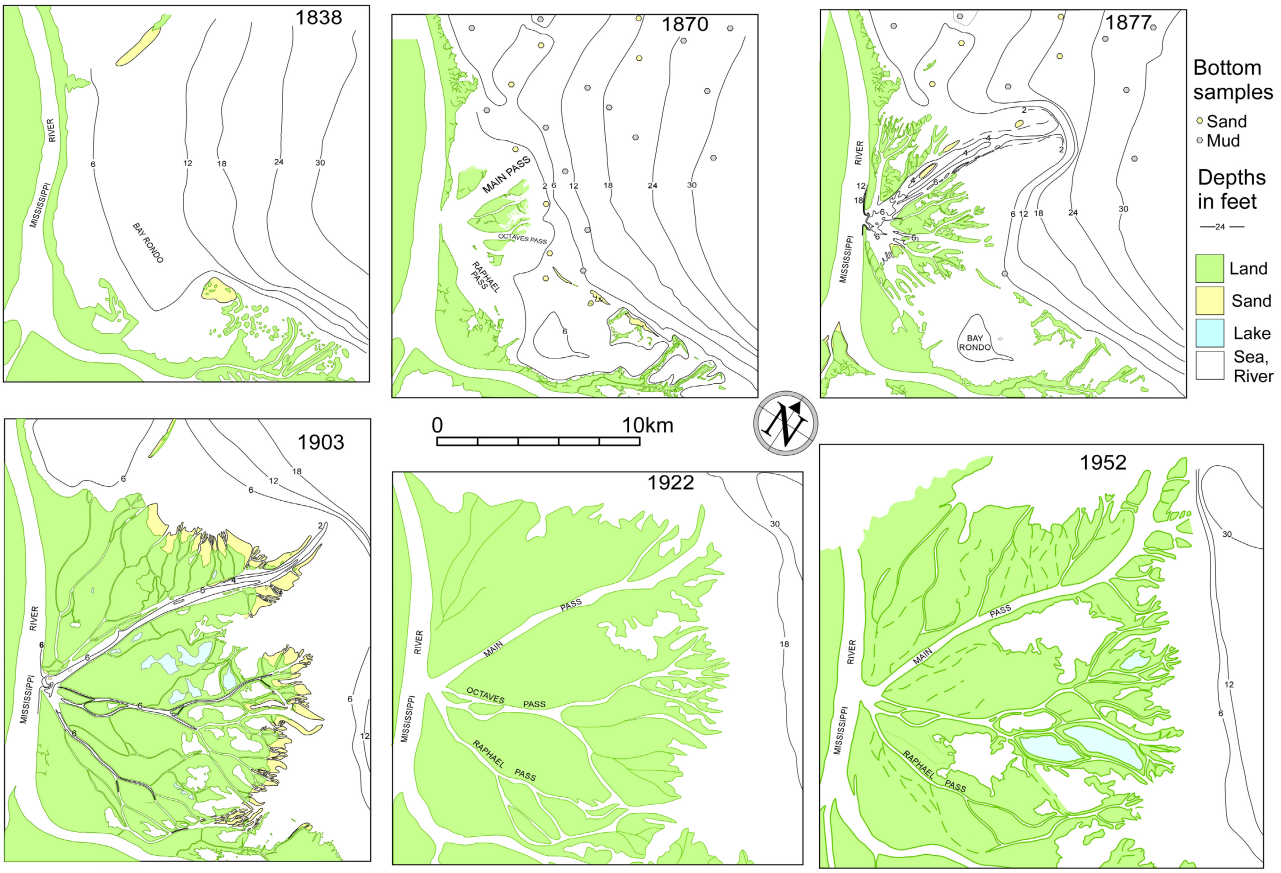

Fig. 8. The Cubit's Gap Crevasse Delta initiated in 1862 near the mouth of the Mississippi River, USA. At first, the delta was characterized by accumulation of a shallow subaqueous sandy platform rather than by a large mouth bar (Welder, 1955). By 1870 the platform had shallowed forcing the flow to cut a suite of channels, three of which persist to the present day. The southern portion of the delta is characterized by numerous channel splits, and by more interdistributary lakes. By contrast, the Main Pass prograded more rapidly with the channel persistently elongating by eroding through river-mouth deposits. The compilation is based on Welder (1955), Wellner *et al.* (2005), and US Coast and Geodetic Survey maps. Depths are in feet. Cubit's Gap is located at 29°11′45.45″N 89°15′49.01″W.

wider, deeper, more flow-efficient channels that would favour continued lobe progradation.

ANOMALOUSLY LONG, STRAIGHT CHANNEL REACHES

Beyond river mouth deposit diversity, anomalously long, straight channel reaches form a second key theme not central to an idealized bifurcation driven model which holds that any given reach length is around seven tenths of its parent reach length. The model is illustrated by stream thread L on the lacustrine Mossy Delta (Fig. 11A; Edmonds & Slingerland, 2007), where, for example, the ratio of lengths for reaches L2 and L3, the reach length ratio, is 0.68. Extending the approach across the same delta, confirms a general decrease in reach length along a series of example distributary threads, with threads L, M, Q and R being well-matched to the model (Fig. 11B). Most reach–length ratios are less than one, with a median value of 0.69 that closely supports the bifurcation-driven model. However, other threads have anomalously long second or third-order reaches. For example, reach O2 is over twice as long as reach L1, and the average ratio is 1.1.

In the bifurcation-driven model, channels lengthen until they split around newly deposited friction-dominated mouth bars. Some long channels may form by avulsion. Others could appear to be overly long if distributaries are abandoned and branch nodes are no longer visible (Figs 8 and 11A). However, examples

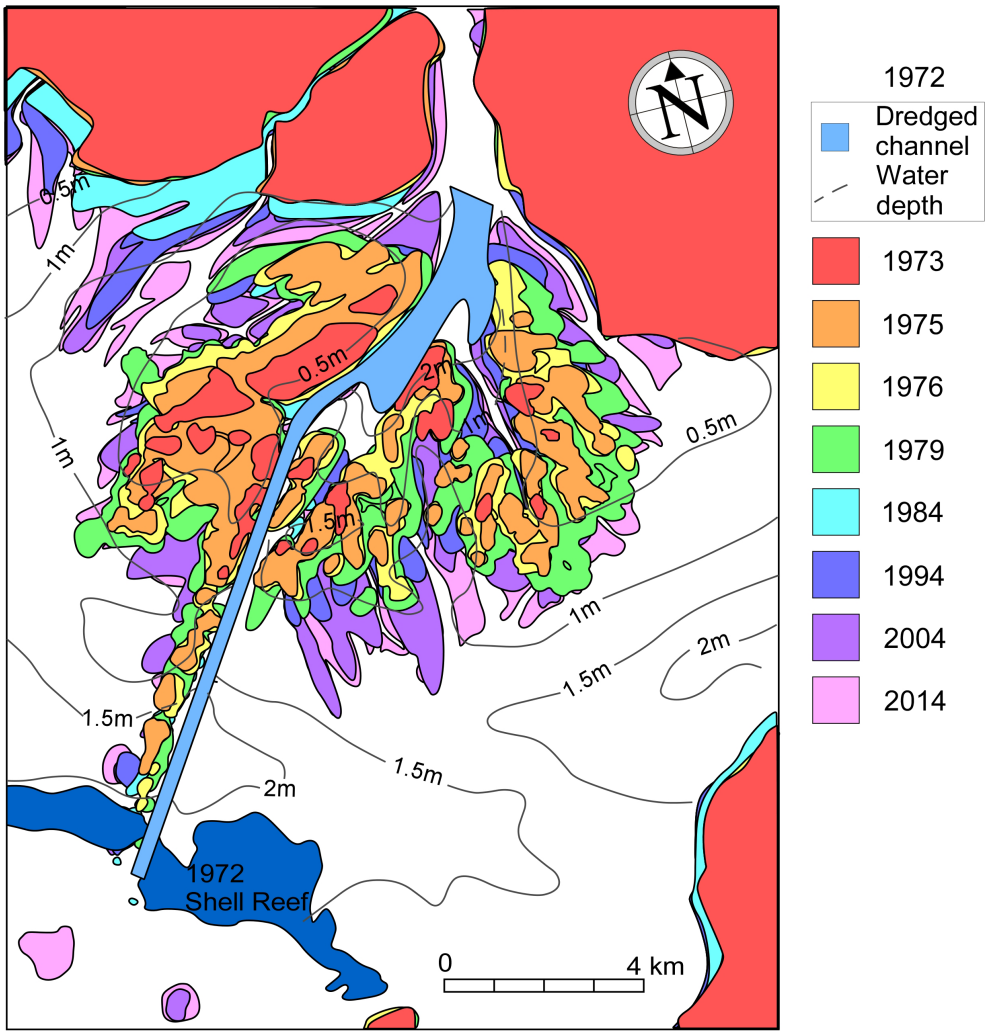

Fig. 9. Coloured polygons capture the subaerial growth of the Atchafalaya Delta, Mississippi, USA. Rather than progressive downstream growth and steady development of smaller mouth bars and channels, the basic form emerged quickly, with subsequent growth being by upstream and downstream accretion and delta-wide. Subaerial portions of the delta are from Van Heerden & Roberts (1988) for 1973 to 1979, and from Google Earth for 1984 to 2014. The outlines of the dredged channel and the shell reef, and 1972 pre-emergence water depths, are from Roberts (1998). The eastern side of the delta is considered relatively unaffected by dredging activities and to have a natural form (Van Heerden & Roberts, 1988). The delta head is located at 29°31′53.33″N 91°26′4.24″W.

presented below suggest that channel elongation is widespread, as a result of: (i) shouldering aside of middle-ground mouth bars; (ii) high-inertia jets forming elongate deltas; (iii) channel extension around abandoned lobes; and (iv) channel extension by flow capture.

Shouldering aside of middle-ground mouth bars

In the bifurcation-driven model, channel splits are expected to be of unequal width, with a ratio of around 1.7 (Edmonds & Slingerland, 2007), but the impact of this observation has not been fully explored. Figure 12 confirms a width ratio of around two for dominant and subordinate reaches on the Wax Lake Delta, and extends the analysis to also distinguish: (i) linking tributary channels that join subordinate and dominant distributary reaches to higher order distributaries; (ii) drainage tributary channels that drain inter-channel islands; and (iii) a tie channel where the sense of flow is equivocal, and may reverse. Assuming that discharge is proportional to the total width of each

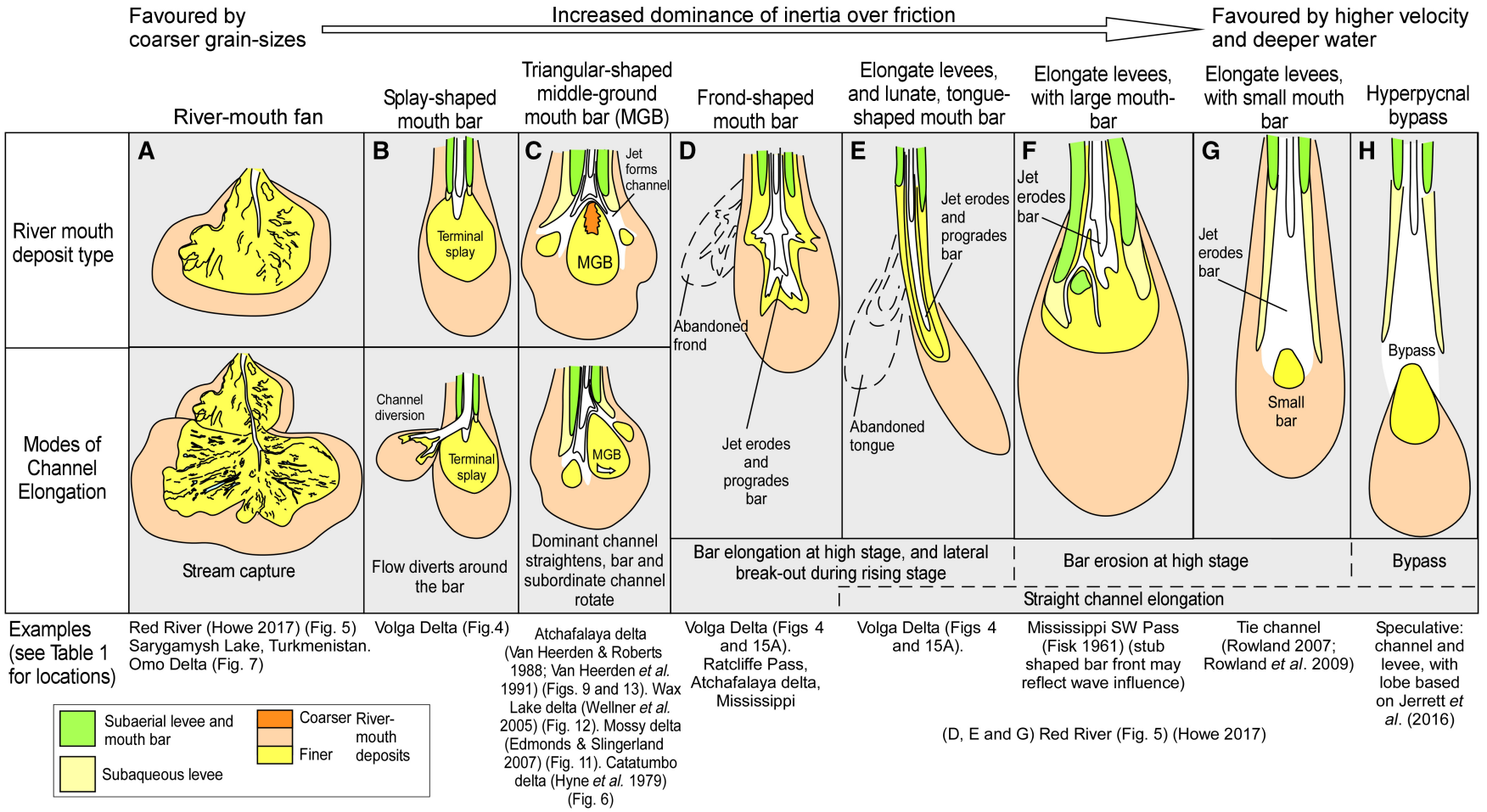

Fig. 10. River-dominated, river-mouth deposits can be arranged conceptually along a spectrum, ranging from friction-dominated river-mouth fans, to inertia-dominated elongate channels. The spectrum can be divided by whether jet flow is spread, split or diverted by river-mouth deposits, or whether jet inertia is high enough to erode them, and/or advect suspended sediment away from the jet centreline, allowing channel elongation. The figure has no implied common scale, and the relative positions of the different river-mouth types on the spectrum is tentative. More elongate forms are hypothesized to reflect higher inertia. Each river mouth deposit type has an associated mode of channel elongation.

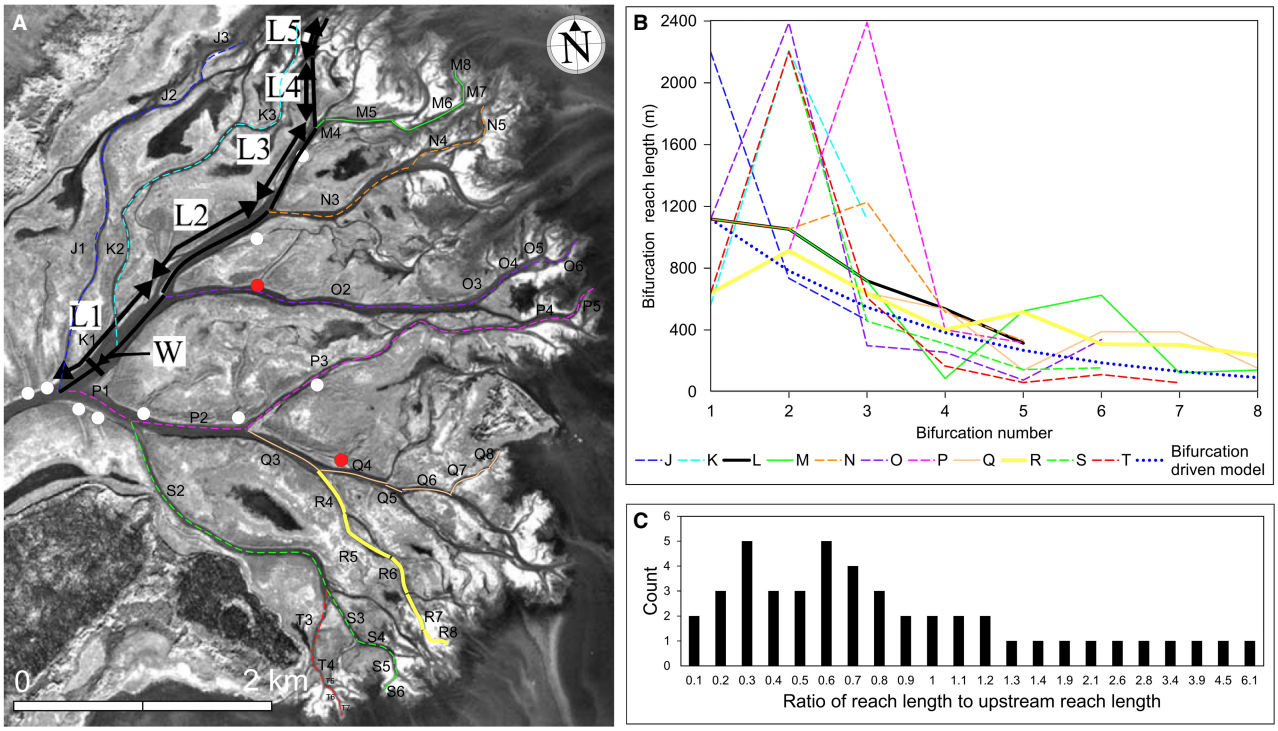

Fig. 11. Reach lengths for selected distributary threads of the lacustrine Mossy Delta, Saskatchewan, Canada. (A) The image and the large font lettering are from Edmonds & Slingerland (2007) who used the L thread to illustrate a steady decrease in reach length down-system (though that is achieved by ignoring the K2 branch). Circles show possible abandoned-channel branch nodes, two of which (red) are confirmed as palaeo-channels by historical maps in Edmonds & Slingerland (2007). (B) Reach length against bifurcation number for 11 channel threads compared against the bifurcation-driven model (dotted line) that daughter reach length is seven tenths of the feeding parent reach length. The L thread, and others, approximate the model but several threads display anomalously long, second and third-order reaches. (C) Histogram of the ratio of daughter to parent reach length for the channel threads documented in (A) and (B). The median value is 0.69, in accordance with the bifurcation-driven model, but there is no unequivocal peak at 0.7, and a mean value of 1.1 emphasizes a large spread and the presence of several anomalously long reaches. The delta head is located at 54°4′9.57″N 102°22′59.00″W.

channel type, then, based on the channel widths measured on Fig. 12, 63% of the channel flow is via the dominant distributaries, 28% via the subordinate distributaries, 7% via the tributaries and 2% via the drainage channels. The estimate is crude because, though measurements on the Cubit's Gap Crevasse Delta suggest that velocity can be constant in distributive channel threads (Esposito *et al.*, 2013), velocity and cross-section shape may vary in other segment types. Furthermore, 23 to 54% of the incoming distributary flux on the Wax Lake Delta enters adjacent islands via minor channels and overbank flow (Hiatt & Passalacqua, 2015; Passalacqua, 2017). Despite these uncertainties, the calculated fluxes suggest that dominant channel segments play the key role in distributing water and sediment.

The growth and impact of dominant and subordinate channel splits around mouth bars has been observed on the adjacent Atchafalaya Delta (Van Heerden *et al.*, 1991). Relatively even initial splits are increasingly marked by asymmetry, so that the dominant channel widens and straightens at the expense of its sister channel which narrows and rotates away from the dominant channel (Fig. 13). The result is a channel split, but one where the dominant channel is a relatively efficient continuation of the primary channel, and it is hypothesized that this may allow the lobe to prograde further than if the channel split was equal, and flow was diverted evenly around a middle-ground, friction-dominated mouth bar. The process is interpreted to have operated on the Catatumbo Delta (Fig. 6) where subordinate splits around mouth bars are eventually abandoned and sealed. Experiments show similar rotation of individual bifurcated channels

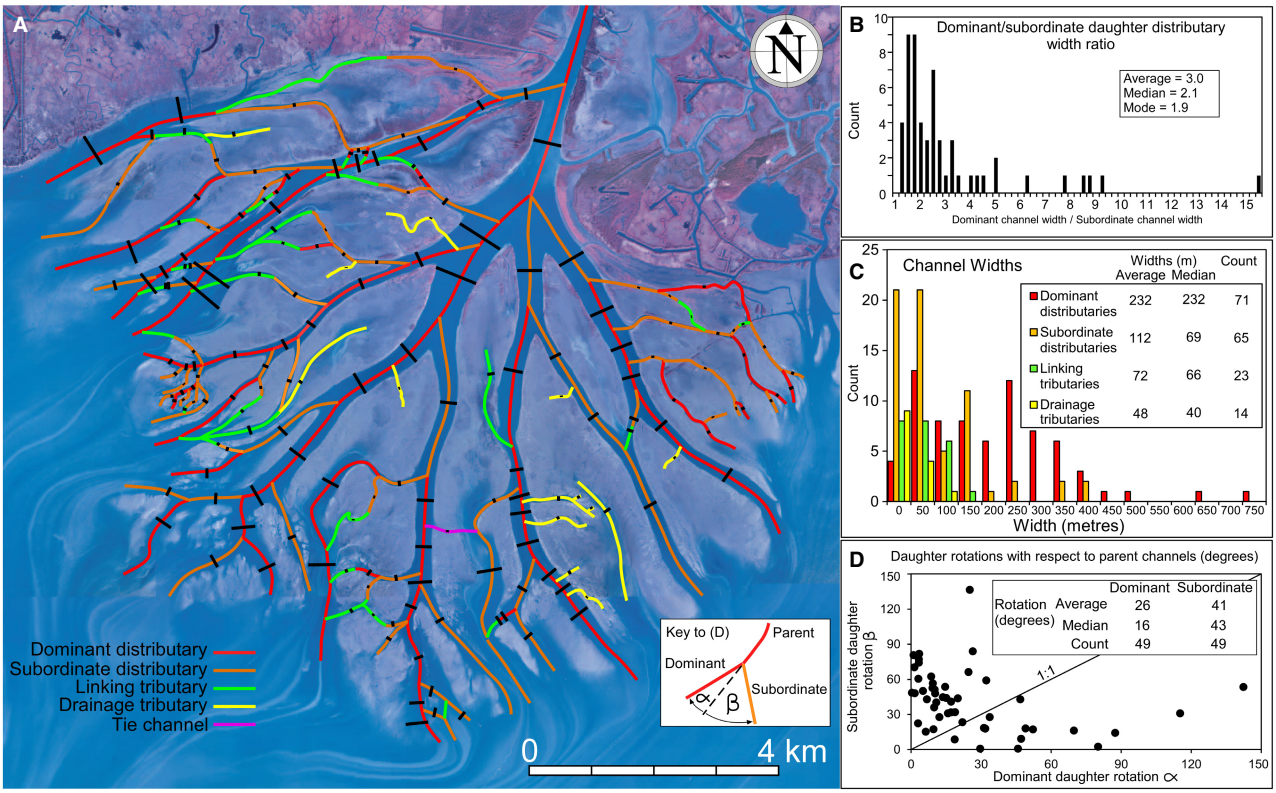

Fig. 12. (A) In distributary systems, assuming that width relates to discharge, at each channel split, wider dominant (red), and narrower subordinate (orange) distributary channel segments can be recognized. Some channel segments merge down system, while others arise locally, allowing linking and drainage tributary segments to be assigned. Black lines give visually representative segment widths. Width data for each segment type show that dominant channel splits are typically twice as wide as their paired subordinate channel (B), and (C) that linking and tributary channel segments are relatively narrow and rare. (D) Dominant daughter channels tend to more closely follow the trend of their parent channel than subordinate daughter channels do. Satellite image of the Wax Lake Delta, Mississippi, USA, from Wellner *et al.* (2005), with the delta head is located at 29°31′53.33″N 91°26′4.24″W.

towards the bar crest and then incision, so that the channel cuts straight across the bar (Daniller-Varghese *et al.*, 2020). Figure 12D suggests that this process may have operated widely across the Wax Lake Delta, as 71% of dominant daughter channels show closer alignment (than subordinate channels) to the trend of parent channels. Systematically preferred orientations of dominant and subordinate channels across a sub-delta, such as shown by the southern distributary of the Catatumbo Delta (where southern channel splits are subordinate; Fig. 6), may reflect tidal currents (Van Heerden *et al.*, 1991; Shaw & Mohrig 2014), wind enhanced river currents, or basin topography boosting hyperpycnal flows in certain directions (Olariu *et al.*, 2012).

Channel progradation by high-inertia jets

High-inertia jets are powerful enough to remove, or cut through, mouth bars, and to form prograding, straight channels and subaqueous levées (Fig. 3). Such channels are the key component of elongate deltas (Fisher, 1969; Kim *et al.*, 2009), i.e. fluvially-dominated deltas, such as the Catatumbo (Fig. 6) with one or two elongate, straight to irregularly sinuous, levéed channels and strong basinward progradation leaving marginal accommodation space unfilled.

Channel extension through abandonment

The Volga Delta plain has a distributive channel pattern with numerous active channel threads (Olariu & Bhattacharya, 2006). The channel pattern developed during forced regression from

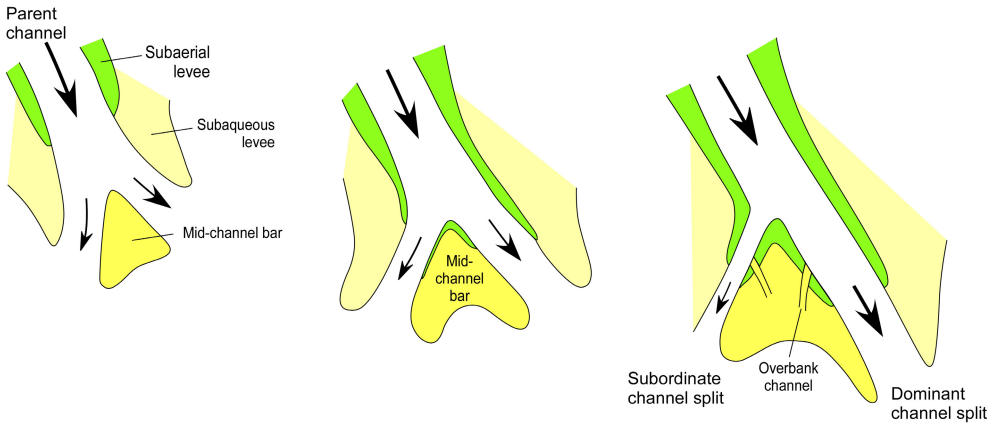

Fig. 13. Friction-dominated middle-ground mouth bars can be 'shouldered aside' by dominant threads when bifurcations around middle-ground mouth bars are unequal. The subordinate channel split narrows, and, along with the mouth bar, rotates away from the line of the parent channel, whereas the dominant channel split extends basinward as a relatively straight continuation of the parent channel (modified from Van Heerden *et al.*, 1991).

the late 1800s to the 1970s (Mikhailov *et al.*, 2012; Chen *et al.*, 2017) accompanied by deposition of a series of elongate sub-deltas, themselves composed of stranded terminal lobes (Fig. 14). Lobes are interpreted to have been abandoned when flow switched from the lobe to elongation of the parent channel, typically around the margin of the latest lobe (Fig. 14B). Each lobe is also elongated basinward, and characterized by one or more dominant threads interpreted to have lengthened through time by combinations of several processes. At river mouths, channels extend by cutting through contemporaneous mouth bars, and by channel elongation due to high-inertia jets (Fig. 15A). At a larger scale, anomalous (increasing) reach lengths on dominant threads within lobes may indicate the abandonment of subordinate distributary branches, and progressive refocus of discharge in to the dominant thread (Fig. 15B and C). The possible influence of base level-fall on lobe elongation and channel extension is addressed in discussion below.

Channel extension by flow capture

Progradation of the Omo River Delta from 2002 to 2018 is accomplished by elongation of three dominant channel threads (Fig. 7). Each is characterized by a sequence of: (i) down-stepping river mouth fans; (ii) lobes composed of friction-dominated mouth-bars; and (iii) elongate channels. The fans and lobes display distributive channel patterns. When each of them is abandoned, rather than avulsing to accommodation space at the fan or lobe margin, flow is captured by a central channel thread that forms a straight continuation of the parent feeder channel, which, in turn, feeds an elongate channel formed by a high-inertia jet. The single thread of the Red River Delta has a similar evolution (Fig. 5).

Summary of elongate channels

Channels elongate when distributive flow is minimized or reduced. For example, in high-inertia jets, such as those that typify tie-channels, well-developed levées prevent distributive flow. With other elongation mechansims, discharge is focussed in to a dominant channel thread as subordinate channels, subordinate channel networks, or lobes are abandoned. The increase in discharge is speculated to result in a deeper more efficient channel that forms longer channel threads, and more elongate lobes. Plots of reach length against reach order (Figs 11 and 15), help test the extent to which delta lobes accord with the bifurcation-driven model. Comparable examples of distibutary networks from the rock record are rare, but are known from high quality 3D seismic data (Zeng *et al.*, 2013). In such cases, reach length–order plots can again be employed, and where they do not correspond closely with the bifurcation-driven model, they may be used to indicate more plausible river-mouth deposits, such as tongue and frond-shaped mouth bars or elongate subaqueous levées rather than middle-ground mouth bars (Fig. 16).

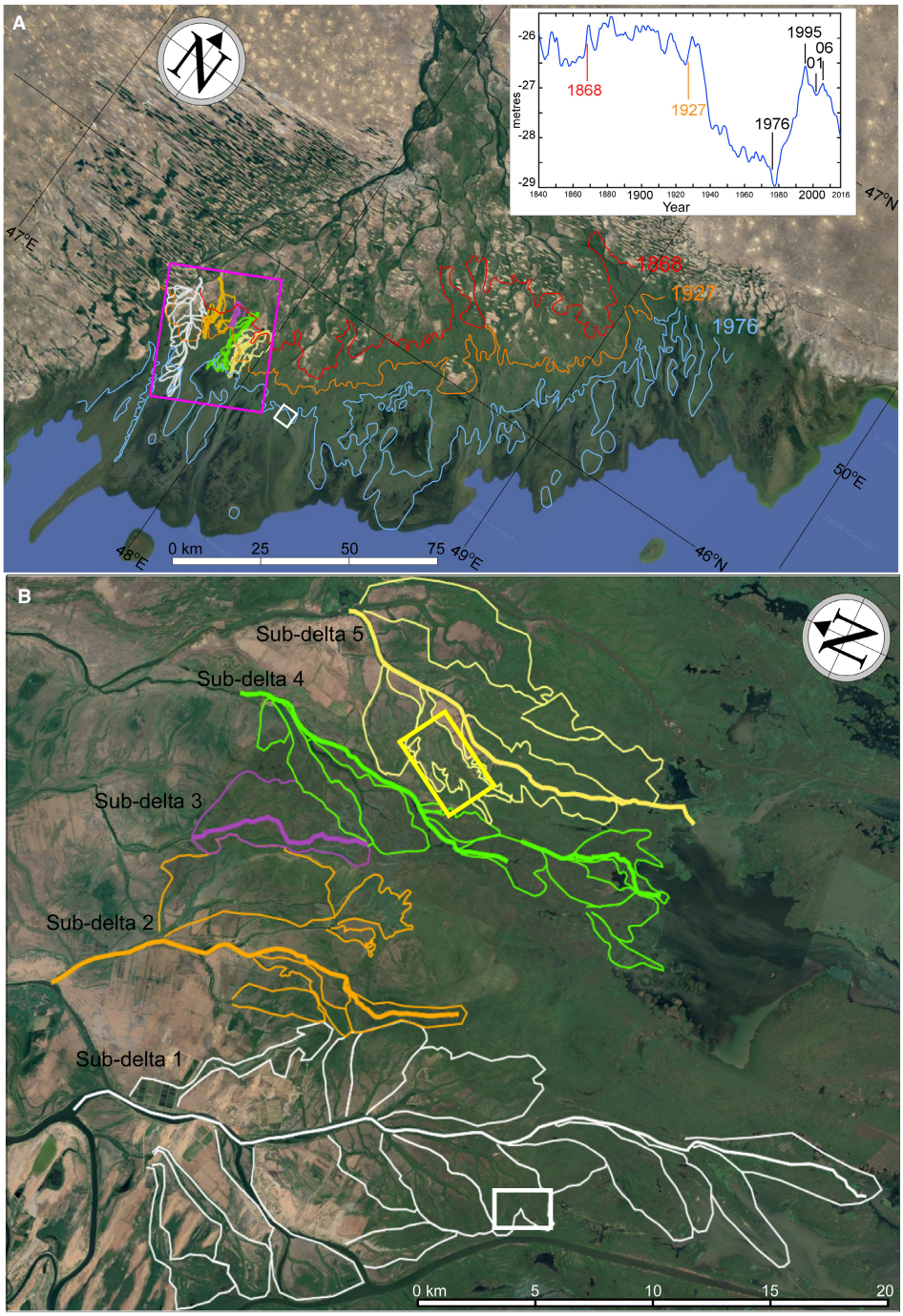

Fig. 14. (A) Satellite view of the Volga Delta showing a distributive channel pattern. The graph (based on Chen *et al.*, 2017) shows how Caspian sea level fell for around a hundred years, resulting in forced regression recorded by historical shoreline positions (simplified from Mikhailov *et al.*, 2012). Satellite image from Google Earth, Image Landsat/Copernicus. The pink rectangle locates (B), and the small white rectangle locates Fig. 4. (B) Detailed analysis of a portion of the delta plain suggests a series of sub-deltas, deposited during sea-level fall. Each sub-delta is interpreted to be composed of a series down-stepping lobes, and a dominant distributary that lengthens as the sub-delta steps basinward, abandoning delta lobes as it does so. In general, dominant channels lengthen by elongating around the most recently deposited lobe. Most lobes are elongate, and characterized by one or more dominant threads that lengthened via a range of processes detailed by images shown on Fig. 15 (located here by white and yellow rectangles). Sub-deltas 3 and 4 form part of the Astrakhan nature reserve described by Overeem *et al.* (2003). Satellite image from Google Earth, Image © 2022 Maxar Technologies, Image Landsat/Copernicus.

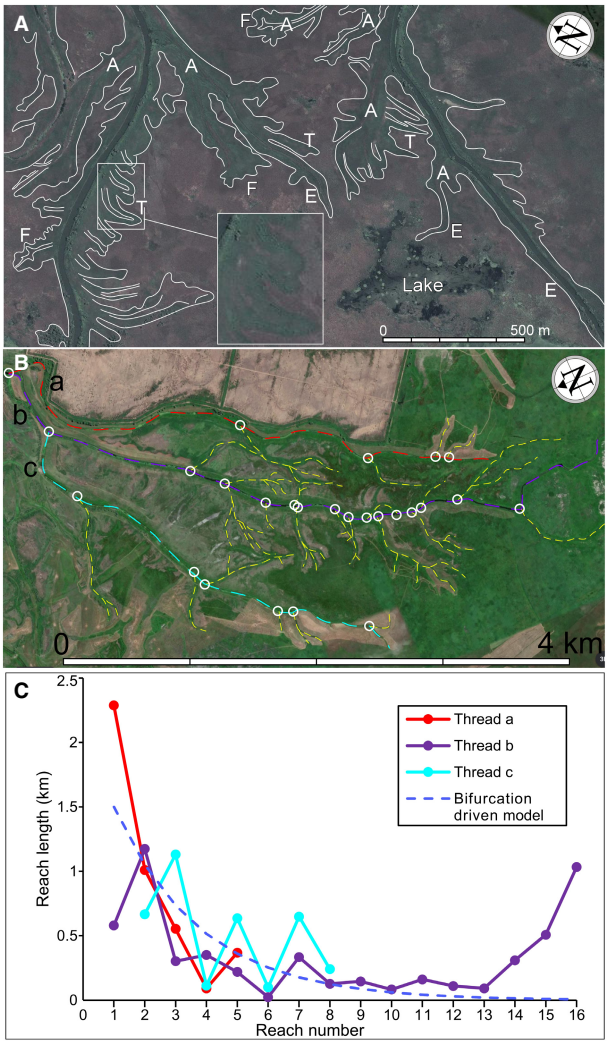

Fig. 15. (A) A range of river-mouth processes appear to have formed elongate channels on this portion of the present-day Volga Delta plain. By direct analogy with Fig. 4, green vegetation is interpreted to record elevated topography reflecting sand and silt with marginal muds. Flow is from the top of the image. Tongue-shaped, T, and frond-shaped, F, mouth bars are interpreted to have been deposited by the left-hand channel thread which appears to have elongated by systematically cutting through the bars. By contrast, the right-hand channel thread elongated without developing significant mouth bar deposits, and is interpreted to reflect channel elongation by levée extension, E. Both channel threads may have extended, in part, by capturing the flow from abandoned subordinate channels, A. The image dates from 2010, was sourced from Google Earth, Image © 2022 Maxar Technologies, and is located on Fig. 14B, at the end of a lobe in the white sub-delta. (B) Three channel threads, a–c, dominate an elongate abandoned delta lobe. The example occurs within sub-delta 5 and is located by the yellow rectangle on Fig. 14B, some 8 km from the present-day delta front. The image dates from 2020, and was sourced from Google Earth, Image © 2020 Maxar Technologies. Each thread formed branches as it extended, and, as shown in (C), channel segments between nodes (white circles) decrease erratically in length until threads a and c die, crudely following the trend of the bifurcation-driven model (Fig. 11) where segment lengths decrease as flow is distributed when channels progressively split, and more than eight orders of bifurcation are rare. Thread b shows a similar pattern until reach 13. However, it subsequently lengthens by addition of extra, progressively longer segments, suggesting that the thread has been rejuvenated. One possibility is that flow that was previously distributed via threads a and c was focussed back in to the dominant b thread as threads a and c were abandoned.

DISCUSSION

Though there has been significant recent progress in the theory and modelling of fluvially-dominated deltas, and, in particular, river-mouth deposits (Fagherazzi *et al.*, 2015), high-quality studies of real-world systems are rare. There are almost no reports of systems over many years with high-quality mapping of landform evolution, monitoring of formative flows and bedforms, records of sediment load, studies of vegetation and biota, and trenching and coring of resulting deposits. As a result, the rare in-depth studies which exist (for example, Van Heerden & Roberts, 1988; Wellner *et al.*, 2005; Rowland, 2007; Cahoon *et al.*, 2011), and the few deltas that have received significant attention (Cubit's Gap, Wax Lake, Atchafalaya, Mississippi Bird Foot), tend to dominate our understanding, and are repeatedly used to benchmark theoretical and modelling studies. River-mouth deposit variability on fluvially-dominated deltas is greater than those studies imply (Fig. 10), but can still be summarized by factors previously recognized to control river-mouth jets (Fagherazzi *et al.*, 2015) – flow inertia, grain size, vegetation and water depth, together with dependent differences in channel depth and width. These factors interact to directly influence river-mouth jets and either: (i) force them to spread, decelerate and deposit material along the jet centreline resulting in channel splitting, diversion or spreading; or (ii) form a vigorous jet that prevents deposition and/or erodes mouth-bar deposits allowing channel elongation.

Although the examples presented here emphasize fluvially-dominated deltas, even weak basin

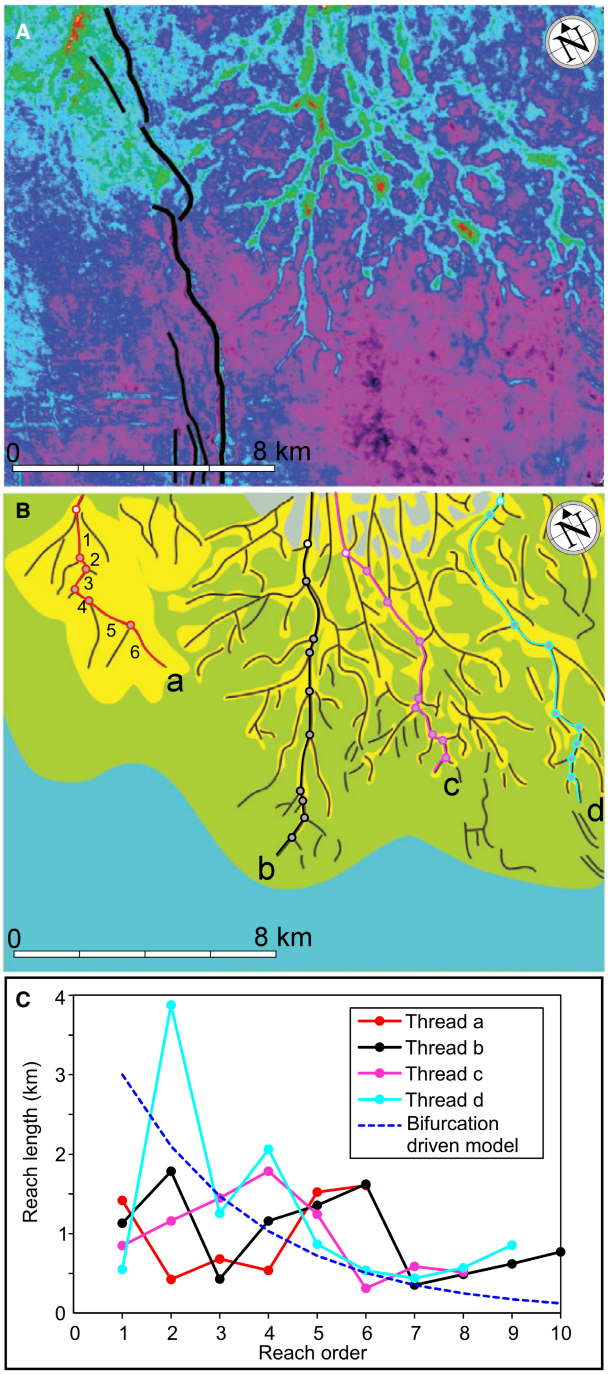

Fig. 16. (A) Three-dimensional seismic stratal slice, (B) interpretation and (C) reach-length plot for threads a–d in lacustrine, river-dominated delta lobes in the Songliao Basin, China – (A) and (B) modified from Zeng *et al.* (2013). Although the branching pattern is clear for each lobe, none of the threads adhere to the bifurcation-driven model shown in the plot. As a result, a suite of river-mouth deposits is suggested: triangular middle-ground mouth bars at branch points; frond and tongue-shaped mouth bars where channels are elongate and the amplitude response is wide and irregular, and elongate levées where the amplitude is narrow and the channels relatively straight.

processes, waves, wind and tides, can influence depositional patterns. For example, though the Wax Lake Delta is widely considered as a type example of a river-dominated delta, and only experiences a small mean tidal range of 0.4 m, at low river-stage, the ebb tide (in conjunction with relatively clear water river flow) results in velocities able to scour through high-stage river-mouth deposits and extend the subaqueous termination of Gadwall Pass, one of the delta's main distributaries (Shaw & Mohrig, 2014). Over time, a distributive terminal pattern transitions to an extended, straight, dominant channel akin to those seen, at a larger scale, where stronger tides operate (Rossi *et al.*, 2016; Lentsch *et al.*, 2018). The same factors are also expressed in larger-scale patterns (Galloway, 1975; Ainsworth *et al.*, 2011), not least because river-mouth processes help set the number and stability of distributary channels (Axelsson, 1967; Orton & Reading, 1993; Olariu & Bhattacharya, 2006; Edmonds & Slingerland, 2007; Caldwell & Edmonds, 2014; Fagherazzi *et al.*, 2015).

Allogenic controls also play a role. For example, base-level changes attendant with sequence stratigraphic cycles, and basin configuration are considered to influence basin processes, with: (i) tides becoming important when deltas are fronted by wide shelf systems, or located in narrow gulfs so that open-ocean tides amplify (Stride, 1982); and (ii) waves being prominent at shelf margins, but dissipated across wide shelves (Reynolds, 1996), and minor when fetch is limited (Tanner, 1971; Komar, 1974; Allen, 1981). As a result, fluvially-dominated deltas are commonly found in sheltered settings protected from waves, or in lakes where fetch is limited, and tides are negligible (Table 1). In addition, flume tank and computer models suggest distributary channel responses to base-level change, with: (i) base-level fall leading to shelf-margin incision that propagates slowly upsystem (Koss *et al.*, 1994) and valley widening with time (Martin *et al.*, 2011); and (ii) higher rates of base-level rise leading to greater channel mobility, more frequent avulsion and smaller sediment bodies (Martin *et al.*, 2009; Liang *et al.*, 2016). However, studies that directly link

models and real-world examples are rare (Rosa *et al.*, 2016). In the examples presented here, the elongate sub-deltas and lobes of the Volga Delta (Fig. 14) may reflect the river mouth 'chasing' a long-term falling lake level. The Omo Delta (Fig. 7) supports this conjecture. It is comparable in size to a Volga sub-delta, associated with lake-level fall, and shows a similar pattern of downstepping delta lobes, incomplete filling of accommodation space and elongation of trunk channels. In the case of the Omo Delta, river-mouth deposit style may also be influenced by base-level changes, as high-friction fans and middle-ground mouth bars are deposited during lake-level fall, whereas elongate, levéed channels developed during subsequent lake-level rise. However, further comparative analysis questions such simple explanations. For example, the Red River Delta, though smaller in scale and deposited during stable/oscillating lake level, has prograded in a similar manner, with an elongate channel, a range of river mouth styles and unfilled marginal accommodation space (Olariu *et al.*, 2012; Fig. 5). Furthermore, though the Volga is similar to the Omo in terms of lake-level fall, very shallow water (<<5 m) and grain size (Table 1), the Volga displays different river-mouth deposit styles, including tongue and frond-shaped mouth bars, and elongate channels, all during overall lake-level fall (Fig. 15). The observations of depositional style varying with base level are intriguing, but too limited to form a general model.

What is clearer is that long-term changes, and wide-ranging effects (such as base-level), cannot explain all river-mouth variability as different river-mouth deposits can occur synchronously and adjacent to one another (Cubit's Gap, Fig. 8; Volga Delta lobe, Fig. 4), and in other cases the examples represent too short a time frame (where known, less than 152 years, Table 1) and too small an area, for long-term, long-wavelength factors (for example, climate change, thermal subsidence) to have played a significant role. In such cases local factors control river mouth variability. Notably fluctuations in discharge associated with river floods may result in river-mouth erosion, channel elongation and deposition of elongate high-inertia mouth bars (for example, tongue-shaped mouth bars) at high stage, and the formation of friction-dominated mouth bars or splays as river stage falls (Fidolini & Ghinassi, 2016; Fig. 4). Similarly, flood variability, may be important with higher peak discharges resulting in higher inertia jets, and longer flood durations resulting in more stable, or more evolved river-mouth deposits (Edmonds & Slingerland, 2007; Shaw *et al.*, 2018). Unequal channel depths and widths, and local substrate variability at river mouths, may also force local jet variability that could be reflected in diverse river-mouth deposits. Local variations in water depth may also play a role. However, water depth alone is not a predictor of river mouth deposit style. Water depth is important in combination with the scale of the jet (large or small), and the degree to which the jet interacts with the basin floor and whether it spreads significantly as a result. The examples in Table 1 illustrate this as (excepting the Mississippi Bird Foot Delta) elongate channels and friction-dominated centreline deposits (for example, middle-ground mouth bars, splay-shaped mouth-bars and high-friction fans) develop in comparable shallow water-depths (Fig. 17).

By using satellite imagery, the present study has broken free of the constraint to study easily accessible deltas, and allowed the analysis of several systems over extended time periods. The diversity of river-mouth deposits, and the suite of channel elongation modes that have emerged was unexpected. The results illustrate features not captured by the bifurcation-driven model (Figs 1 and 2), emphasize the selective abandonment of subordinate channel patterns and reaches, with flow reverting to dominant threads thereby fostering progradation, and suggest a broader range of possible interpretations for long channel reaches, for river-mouth elements and for their lateral variability. However, by the standards set out above, the study cannot claim to be either detailed or complete.L

1 Continued analysis may increase or refine the range of river-mouth deposits and the known mechanisms for channel elongation.

2 The analysis has focussed on the sandy portion of river-mouth deposits, the larger, mud-prone part, more likely to be moved by basin currents and deposited from plumes (Roberts, 1998), has not been addressed.

3 Almost all of the case studies would benefit from fieldwork, in particular to confirm interpretations based largely on satellite imagery and to describe the sedimentary record of each river-mouth deposit style, and so bridge the gap between plan forms described here and the rock record. For example, possible links between the diverse plan-form types described here and the steeper clinoforms seen in many ancient

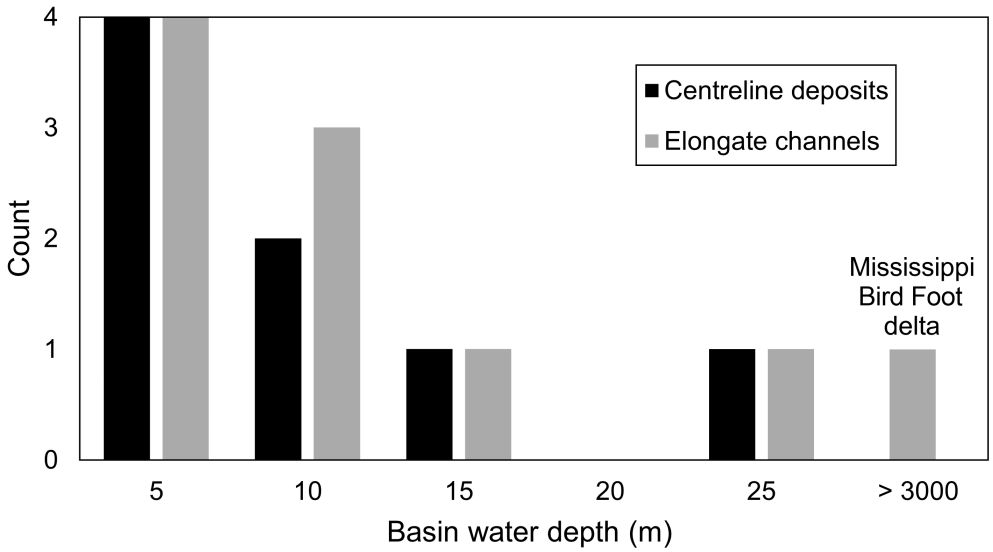

Fig. 17. Water depth is an important control on river mouth deposit type, as when jets impinge on the basin floor they are forced to expand, decelerate and deposit sediment on the jet centreline. However, though the available water-depth data are somewhat crude, the examples on Table 1 suggest that water depth alone is not a predictor of river-mouth deposit style as centreline deposits (middle-ground mouth bars, splay-shaped mouth bars and river-mouth fans) occur in similar water depths to elongate channels.

examples (Panther Tongue 1°–8°; Olariu & Bhattacharya, 2006; Ferron 1°–7°, Howell *et al.*, 2008, Ahmed *et al.*, 2014; Xert Formation 7°–24° Cole *et al.*, 2020) are unexplored. Similarly, Fidolini & Ghinassi (2016) provide the only known descriptions comparable to the tongue and splay-shaped mouth bars documented here. Fieldwork is also required to determine local controls on river-mouth deposit variability, both laterally, and over time. For instance, monitoring of the active Volga Delta front (Fig. 4) to confirm formative conditions for tongue, frond and splay-shaped mouth bars would be invaluable.

4 More numerous, and longer-term studies with richer records of, for example, lake level, river discharge and sediment load are required to establish the influence of allogenic factors, such as base level and climate change, on river-mouth deposits.

5 Focussed computer and flume modelling studies are likely to offer complementary insights to fieldwork – as much as those approaches may be refined by comparing them with the examples presented here.

Despite the wide scope for further work, the diversity of river-mouth deposits and the range of mechanisms of channel elongation that have been documented here is notable. The examples provide a glimpse at alternative, new ways of interpreting ancient river-dominated deltaic successions, and suggest a wider range of possible outcomes for projects that divert flow and/or cut channels to create new land.

CONCLUSIONS

Well-known examples of fine-grained, shallow-water, fluvially-dominated deltas of the Mississippi River, and elsewhere, suggest rather uniform river-mouth jets. On lobate deltas lower inertia jets are considered to form self-similar, middle-ground mouth bars that split flows and result in progressively smaller bars and narrower, shorter channels as progradation proceeds, and, in a similar way, elongate deltas are marked by channel elongation reflecting a persistent high-inertia jet style. By contrast, review of some previous studies, and satellite imagery of less well-known, fluvially-dominated deltas, suggests a suite of mechanisms by which elongate channels may form, and reveals diverse river-mouth deposits, within individual lobes, between lobes and along the length of elongate channels, suggesting that spatial and temporal jet variability can be common.

In addition to high-inertia jets, delta head and backwater avulsion, elongate channel threads may also form: (i) as dominant-channel splits grow and shoulder aside mouth bars, and

subordinate splits wither and die; and (ii) when subordinate distributary networks are abandoned, and flow returns to rejuvenate a dominant parent channel thread.

River-mouth deposits range from fans, via splay, triangular middle-ground, frond and tongue shaped-mouth bars, to elongate channels with prominent subaqueous levées (Fig. 10). The suite of forms is interpreted to reflect a spectrum of jets that can be divided in to two by whether: (i) sediments deposited along the jet centreline force the jet to spray, split or divert; or (ii) inertia is sufficient for the jet to erode the deposits and to elongate the parent channel. Higher-inertia flows are thought likely to favour more elongate river-mouth deposits.

The variety of river-mouth deposits, within and between lobes suggests that, in combination, controlling factors such as water depth, substrate, sediment load, channel geometry, and perhaps in particular discharge, can vary significantly across and between individual delta lobes. Similarly, the wider range of mechanisms described here that operate to elongate distributary channels, fostering lobe elongation and continued progradation, may at times balance the tendency for the creation of ever more inefficient channel bifurcations that lead to lobe switching.

The examples presented here have shown that individual, real-world, fluvially-dominated deltas and delta lobes are characterized by a range of river-mouth deposits, both laterally and over time. However, spatial and temporal variations of river-mouth deposits, and the mechanisms by which distributary channels can elongate, are not generally included in models of fluvially-dominated deltas for resource management of the subsurface, nor in models of modern deltas employed in land remediation. Yet this variability may be critical in many examples. A revised model to describe the development of fluvially-dominated deltas and delta lobes is required. The model is likely to be based on river mouth jet dynamics, and to build on the bifurcation-driven model and its extension in numerical and simulation studies that already explain a suite of diverse river mouth styles (Canestrelli *et al.*, 2014; Fagherazzi *et al.*, 2015). Ideally, the model will also predict the channel elongation mechanisms and the details of the modern river-mouth deposits illustrated here, when they develop, their scale, proportions and spacing at the lobe and delta scale.

ACKNOWLEDGEMENTS

I gratefully acknowledge a previous honorary position at the University of Aberdeen, and thank John Howell and Martin Wells for comments on an early version of the manuscript. I am grateful too to journal reviewers, Brian Willis and two anonymous reviewers, for their detailed comments and suggestions, and appreciate the patient guidance of editors Piret Plink-Björklund and Jeff Peakall.

REFERENCES

Abd-Elaty, I., **Sallam, G.A.**, **Straface, S.** and **Scozzari, A.** (2019) Effects of climate change on the design of subsurface drainage systems in coastal aquifers in arid/semi-arid regions: case study of the Nile delta. *Sci. Total Environ.*, **672**, 283–295. https://doi.org/10.1016/j.scitotenv.2019.03.483

Ahmed, K.M., **Bhattacharya, P.**, **Hasan, M.A.**, **Akhter, S.H.**, **Alam, S.M.**, **Bhuyian, M.H.**, **Imam, M.B.**, **Khan, A.A.** and **Sracek, O.** (2004) Arsenic enrichment in groundwater of the alluvial aquifers in Bangladesh: an overview. *Appl. Geochem.*, **19**, 181–200. https://doi.org/10.1016/j.apgeochem.2003.09.006

Ahmed, S., **Bhattacharya, J.P.**, **Garza, D.E.** and **Li, Y.** (2014) Facies architecture and stratigraphic evolution of a river-dominated delta front, Turonian Ferron Sandstone, Utah, USA. *J. Sed. Res.*, **84**, 97–121. https://doi.org/10.2110/jsr.2014.6

Ainsworth, R.B., **Vakarelov, B.K.**, **Eide, C.H.**, **Howell, J.A.** and **Bourget, J.** (2019) Linking the high-resolution architecture of modern and ancient wave-dominated deltas: processes, products, and forcing factors. *J. Sediment. Res.*, **89**, 168–185. https://doi.org/10.2110/jsr.2019.7

Ainsworth, R.B., **Vakarelov, B.K.** and **Nanson, R.A.** (2011) Dynamic spatial and temporal prediction of changes in depositional processes on clastic shorelines: toward improved subsurface uncertainty reduction and management. *AAPG Bull.*, **95**, 267–297. https://doi.org/10.1306/06301010036

Alexander, J.S., **Wilson, R.C.** and **Green, W.R.** (2012) A brief history and summary of the effects of river engineering and dams on the Mississippi River system and delta: U.S. Geol. Surv. Circular 1375. 43 pp. https://pubs.usgs.gov/circ/1375/

Allen, P.A. (1981) Wave-generated structures in the Devonian lacustrine sediments of south-east Shetland and ancient wave conditions. *Sedimentology*, **28**, 369–379. https://doi.org/10.1111/j.1365-3091.1981.tb01686.x

Andrén, H. (1994). Development of the Laitaure delta, Swedish Lappland: A study of growth, distributary forms and processes. Doctoral dissertation, Uppsala University. 188 pp.

Axelsson, V. (1967) The Laitaure Delta: A study of deltaic morphology and processes. *Geogr. Ann. Ser. A Phys. Geography*, **49**, 1–127. https://doi.org/10.2307/520865

Bates, C.C. (1953) Rational theory of delta formation. *AAPG Bull.*, **37**, 2119–2162. https://doi.org/10.1306/5CEADD76-16BB-11D7-8645000102C1865D

Belevich, E.F. (1956) About the history of the Volga Delta. (In Russian). *Rep. Oceanol. Commun.*, **1**, 37–56.

Bergillos, R.J., **López-Ruiz, A.**, **Principal-Gómez, D.** and **Ortega-Sánchez, M.** (2018) An integrated methodology to forecast the efficiency of nourishment strategies in eroding deltas. *Sci. Total Environ.*, **613**, 1175–1184. https://doi.org/10.1016/j.scitotenv.2017.09.197

Bomer, E.J., **Bentley, S.J.**, **Hughes, J.E.**, **Wilson, C.A.**, **Crawford, F.** and **Xu, K.** (2019) Deltaic morphodynamics and stratigraphic evolution of Middle Barataria Bay and Middle Breton Sound regions, Louisiana, USA: implications for river-sediment diversions. *Est. Coast. Shelf. Sci.*, **224**, 20–33. https://doi.org/10.1016/j.ecss.2019.03.017

Butzer, K.W. (1970) Contemporary depositional environments of the Omo Delta. *Nature*, **226**, 425–430. https://doi.org/10.1038/226425a0

Caldwell, R.L. and **Edmonds, D.A.** (2014) The effects of sediment properties on deltaic processes and morphologies: a numerical modelling study. *J. Geophys. Res. Earth Surf.*, **119**, 961–982. https://doi.org/10.1002/2013JF002965

Cahoon, D.R., **White, D.A.** and **Lynch, J.C.** (2011) Sediment infilling and wetland formation dynamics in an active crevasse splay of the Mississippi River delta. *Geomorphology*, **131**, 57–68. https://doi.org/10.1016/j.geomorph.2010.12.002

Campbell, J.B. and **Wynne, R.H.** (2011) *Introduction to Remote Sensing*, 5th edn. Guilford Press, New York.

Canestrelli, A., **Nardin, W.**, **Edmonds, D.**, **Fagherazzi, S.** and **Slingerland, R.** (2014) Importance of frictional effects and jet instability on the morphodynamics of river mouth bars and levees. *J. Geophys. Res. Oceans*, **119**, 509–522. https://doi.org/10.1002/2013JC009312

Carr, C.J. (2017) *River Basin Development and Human Rights in Eastern Africa—A Policy Crossroads*, p. 240. Springer Nature, Cham. https://doi.org/10.1007/978-3-319-50469-8

Chen, J.L., **Pekker, T.**, **Wilson, C.R.**, **Tapley, B.D.**, **Kostianoy, A.G.**, **Cretaux, J.F.** and **Safarov, E.S.** (2017) Long-term Caspian Sea level change. *Geophys. Res. Lett.*, **44**, 6993–7001. https://doi.org/10.1002/2017GL073958

Cole, G., **Jerrett, R.** and **Watkinson, M.P.** (2020) A stratigraphic example of the architecture and evolution of shallow water mouth bars. *Sedimentology*, **68**, 1–28. https://doi.org/10.1111/sed.12825

Coleman, J.M. and **Gagliano, S.M.** (1964) Cyclic sedimentation in the Mississippi River deltaic plain. *Gulf Coast Assoc. Geol. Societ. Trans.*, **14**, 67–80.

Coffey, T.S. and **Shaw, J.B.** (2017) Congruent bifurcation angles in river delta and tributary channel networks. *Geophys. Res. Lett.*, **44**, 11–427. https://doi.org/10.1002/2017GL074873

Crapper, P.F. (1977) Forced plume characteristics. *Tellus*, **29**, 470–475. https://doi.org/10.1111/j.2153-3490.1977.tb00758.x

Custodio, E. (2010) Coastal aquifers of Europe: an overview. *Hydrogeol. J.*, **18**, 269–280. https://doi.org/10.1007/s10040-009-0496-1

Daniller-Varghese, M.S., **Kim, W.** and **Mohrig, D.C.** (2020) The effect of flood intermittency on bifurcations in fluviodeltaic systems: Experiment and theory. *Sedimentology*, **67**, 3055–3066. https://doi.org/10.1111/sed.12732

Edmonds, D. A., **Slingerland, R. L.** and **Desibour, R. M.** (2004) Geometric properties of bifurcating delta distributary channels. Am. Geophys. Union Publ. Fall Meeting Abstracts, H43A-0367.

Edmonds, D.A. and **Slingerland, R.L.** (2007) Mechanics of river mouth bar formation: implications for the morphodynamics of delta distributary networks. *J. Geophys. Res. Earth Surface*, **112**, 1–14. https://doi.org/10.1029/2006JF000574

Edmonds, D.A., **Hoyal, D.C.**, **Sheets, B.A.** and **Slingerland, R.L.** (2009) Predicting delta avulsions: implications for coastal wetland restoration. *Geology*, **37**, 759–762. https://doi.org/10.1130/G25743A.1

Edmonds, D.A. and **Slingerland, R.L.** (2010) Significant effect of sediment cohesion on delta morphology. *Nat. Geosci.*, **3**, 105–109. https://doi.org/10.1038/ngeo730

Edmonds, D.A., **Paola, C.**, **Hoyal, D.C.** and **Sheets, B.A.** (2011) Quantitative metrics that describe river deltas and their channel networks. *J. Geophys. Res. Earth Surface*, **116**, 1–15. https://doi.org/10.1029/2010JF001955

Edmonds, D.A., **Caldwell, R.L.**, **Brondizio, E.S.** and **Siani, S.M.** (2020) Coastal flooding will disproportionately impact people on river deltas. *Nat. Commun.*, **11**, 1–8. https://doi.org/10.1038/s41467-020-18531-4

Elliott, T. (1976) Upper Carboniferous sedimentary cycles produced by river-dominated, elongate deltas. *J. Geol. Soc. London*, **132**, 199–208. https://doi.org/10.1144/gsjgs.132.2.0199

Ericson, J.P., **Vörösmarty, C.J.**, **Dingman, S.L.**, **Ward, L.G.** and **Meybeck, M.** (2006) Effective sea-level rise and deltas: causes of change and human dimension implications. *Glob. Planet. Change*, **50**, 63–82. https://doi.org/10.1016/j.gloplacha.2005.07.004

Esposito, C.R., **Georgiou, I.Y.** and **Kolker, A.S.** (2013) Hydrodynamic and geomorphic controls on mouth bar evolution. *Geophys. Res. Lett.*, **40**, 1540–1545. https://doi.org/10.1002/grl.50333

Fagherazzi, S., **Edmonds, D.A.**, **Nardin, W.**, **Leonardi, N.**, **Canestrelli, A.**, **Falcini, F.**, **Jerolmack, D.J.**, **Mariotti, G.**, **Rowland, J.C.** and **Slingerland, R.L.** (2015) Dynamics of river mouth deposits. *Rev. Geophys.*, **53**, 642–672. https://doi.org/10.1002/2014RG000451

Falcini, F. and **Jerolmack, D.J.** (2010) A potential vorticity theory for the formation of elongate channels in river deltas and lakes. *J. Geophys. Res. Earth Surface*, **115**, 1–18. https://doi.org/10.1029/2010JF001802

Fisher, W.L. (1969) Facies characterization of Gulf Coast Basin delta systems, with some Holocene analogues. *Trans. Gulf Coast Assn. Geol. Soc.*, **XIX**, 239–261.

Fidolini, F. and **Ghinassi, M.** (2016) Friction-and inertia-dominated effluents in a lacustrine, river-dominated deltaic succession (Pliocene upper Valdarno Basin, Italy). *J. Sedim. Res.*, **86**, 1083–1101. https://doi.org/10.2110/jsr.2016.65

Fisk, H.N. (1961) Bar-finger sands of Mississippi delta. In: *Geometry of Sandstone Bodies* (Eds Peterson, J.A. and Osmond, J.C.), Vol. **22**, pp. 29–52. *AAPG Spec. Publ.* AAPG, Tulsa.

Fielding, C.R., **Trueman, J.D.** and **Alexander, J.** (2005) Sharp-based, flood-dominated mouth bar sands from the Burdekin River Delta of north-eastern Australia: extending the spectrum of mouth-bar facies, geometry, and stacking patterns. *J. Sed. Res.*, **75**, 55–66. https://doi.org/10.2110/jsr.2005.006

Flint, S., **Stewart, D.J.** and **Van Riessen, E.D.** (1989) Reservoir geology of the Sirikit oilfield, Thailand: lacustrine deltaic sedimentation in a Tertiary intermontane basin. In: *Deltas: Sites and Traps for Fossil Fuels* (Eds Whateley, M.K.G. and Pickering, K.T.), Vol. **41**, pp. 223–235. *Geol. Soc. London Spec. Publ.* The Geological Society, London. https://doi.org/10.1144/GSL.SP.1989.041.01.16

Galloway, W.E. (1975) Process framework for describing the morphologic and stratigraphic evolution of deltaic depositional systems. In: *Deltas, Models for Exploration* (Ed Broussard, M.L.), pp. 87–98. Geological Society, Houston.

Geleynse, N., **Storms, J.E.**, **Walstra, D.J.R.**, **Jagers, H.A.**, **Wang, Z.B.** and **Stive, M.J.** (2011) Controls on river delta formation; insights from numerical modelling. *Earth Planet. Sci. Lett.*, **302**, 217–226. https://doi.org/10.1016/j.epsl.2010.12.013

Giosan, L., **Donnelly, J.P.**, **Vespremeanu, E.**, **Bhattacharya, J.P.**, **Olariu, C.** and **Buonaiuto, F.S.** (2005) River delta morphodynamics: Examples from the Danube delta. In: *River Deltas-Concepts, Models, and Examples* (Eds Giosan, L. and Bhattacharya, J.P.), Vol. **83**, pp. 393–411. *SEPM Spec. Publ.* SEPM, Tulsa.

Giosan, L., **Syvitski, J.**, **Constantinescu, S.** and **Day, J.** (2014) Climate change: Protect the world's deltas. *Nat. News*, **516**, 31. https://doi.org/10.1038/516031a

Haasnoot, M., **Middelkoop, H.**, **Offermans, A.**, **Van Beek, E.** and **Van Deursen, W.P.** (2012) Exploring pathways for sustainable water management in river deltas in a changing environment. *Clim. Change*, **115**, 795–819. https://doi.org/10.1007/s10584-012-0444-2

Hampson, G. J., **Reynolds, A. D.**, **Kostic, B.** and **Wells, M. R.** (2017) Introduction to the sedimentology of paralic reservoirs: recent advances. *Geol. Soc. London Spec. Publ.*, **444**, 426. https://doi.org/10.1144/SP444.14

Harris, J.P. (1989) The sedimentology of a Middle Jurassic lagoonal delta system: Elgol Formation (Great Estuarine Group), NW Scotland. In: *Deltas: Sites and Traps for Fossil Fuels* (Eds Whateley, M.K.G. and Pickering, K.T.), Vol. **41**, pp. 147–166. *Geol. Soc. London Spec. Publ.* The Geological Society, London. https://doi.org/10.1144/GSL.SP.1989.041.01.12

Hartley, A.J., **Weissmann, G.S.** and **Scuderi, L.** (2017) Controls on the apex location of large deltas. *J. Geol. Soc. London*, **174**, 10–13. https://doi.org/10.1144/jgs2015-154

Hiatt, M. and **Passalacqua, P.** (2015) Hydrological connectivity in river deltas: The first-order importance of channel-island exchange. *Water Resour. Res.*, **51**, 2264–2282. https://doi.org/10.1002/2014WR016149

Higgins, S.A. (2016) Advances in delta-subsidence research using satellite methods. *Hydrogeol. J.*, **24**, 587–600. https://doi.org/10.1007/s10040-015-1330-6

Howell, J., **Vassel, Å.** and **Aune, T.** (2008) Modelling of dipping clinoform barriers within deltaic outcrop analogues from the Cretaceous Western Interior Basin, USA. In: *Modelling in Hydrocarbon Development* (Eds Robinson, A., Griffiths, P., Price, S., Hegre, J. and Muggeridge, A.), Vol. **309**, pp. 99–121. *Geol. Soc. London Spec. Publ.* The Geological Society, London. https://doi.org/10.1144/SP309.8

Howe, T. (2017) The evolution and stratigraphic architecture of fluvio-lacustrine deltas: reservoir characteristics from the Red River Delta, Lake Texoma and the Denton Creek Delta, Grapevine Lake. Texas Christian University thesis, 76 pp.

Hoyal, D.C.J.D. and **Sheets, B.A.** (2009) Morphodynamic evolution of experimental cohesive deltas. *J. Geophys. Res. Earth Surf.*, **114**, 1–18. https://doi.org/10.1029/2007JF000882

Holle, C.G. (1951) Sedimentation at the mouth of the Mississippi river. *Coast. Eng. Proceed.*, **1**, 111–129. https://doi.org/10.9753/icce.v2.10

Huling, G., and **Holbrook, J.** (2016) Clustering of elongate muddy delta lobes within fluviolacustrine systems, Jurassic Kayenta Formation, Utah. In: *Autogenic Dynamics and Self-Organization in Sedimentary Systems* (Eds **D. A. Budd**, **E. A. Hajek** and **S. J. Purkis**), *SEPM Spec. Publ.*, **106**, 145-162. SEPM, Tulsa. https://doi.org/10.2110/sepmsp.106.11

Hyne, N.J., **Cooper, W.A.** and **Dickey, P.A.** (1979) Stratigraphy of intermontane, lacustrine delta, Catatumbo river, Lake Maracaibo, Venezuela. *AAPG Bull.*, **63**, 2042–2057. https://doi.org/10.1306/2F918860-16CE-11D7-8645000102C1865D

Jerolmack, D.J. and **Swenson, J.B.** (2007) Scaling relationships and evolution of distributary networks on wave-influenced deltas. *Geophys. Res. Lett.*, 1–5. https://doi.org/10.1029/2007GL031823

Jerolmack, D.J. (2009) Conceptual framework for assessing the response of delta channel networks to Holocene sea level rise. *Quatern. Sci. Rev.*, **28**, 1786–1800. https://doi.org/10.1016/j.quascirev.2009.02.015

Jerrett, R.M., **Bennie, L.I.**, **Flint, S.S.** and **Greb, S.F.** (2016) Extrinsic and intrinsic controls on mouth bar and mouth bar complex architecture: examples from the Pennsylvanian (Upper Carboniferous) of the central Appalachian Basin, Kentucky, USA. *Geol. Soc. Am. Bull.*, **128**, 1696–1716. https://doi.org/10.1130/B31429.1

Kim, W., **Dai, A.**, **Muto, T.** and **Parker, G.** (2009) Delta progradation driven by an advancing sediment source: coupled theory and experiment describing the evolution of elongated deltas. *Wat. Resour. Res.*, **45**, 1–16. https://doi.org/10.1029/2008WR007382

Komar, P.D. (1974) Oscillatory ripple marks and the evaluation of ancient wave conditions and environments. *J. Sed. Res.*, **44**, 169–180. https://doi.org/10.1306/74D729B4-2B21-11D7-8648000102C1865D

Koss, J.E., **Ethridge, F.G.** and **Schumm, S.A.** (1994) An experimental study of the effects of base-level change on fluvial, coastal plain and shelf systems. *J. Sed. Res.*, **64**, 90–98. https://doi.org/10.1306/D4267F64-2B26-11D7-8648000102C1865D

LACPRA (2017) Louisiana's Comprehensive Master Plan for a Sustainable Coast, Baton Rouge, LA. Coastal Protection and Restoration Authority of Louisiana, 93 pp.

Lang, J., **Fedele, J.**, and **Hoyal, D.** (2019) Bedform successions formed by submerged plane-wall jet flows. Marine and River Dune Dynamics – MARID VI, 151-156

Lauria, V., **Das, I.**, **Hazra, S.**, **Cazcarro, I.**, **Arto, I.**, **Kay, S.**, **Ofori-Danson, P.**, **Ahmed, M.**, **Hossain, M.A.**, **Barange, M.** and **Fernandes, J.A.** (2018) Importance of fisheries for food security across three climate change vulnerable deltas. *Sci. Total Environ.*, **640**, 1566–1577. https://doi.org/10.1016/j.scitotenv.2018.06.011

Lentsch, N., **Finotello, A.** and **Paola, C.** (2018) Reduction of deltaic channel mobility by tidal action under rising relative sea level. *Geology*, **46**, 599–602. https://doi.org/10.1130/G45087.1

Lin, W. and **Bhattacharya, J.P.** (2021) Storm-flood-dominated delta: a new type of delta in stormy oceans. *Sedimentology*, **68**, 1109–1136. https://doi.org/10.1111/sed.12819

List, E.J. (1982) Turbulent jets and plumes. *Annu. Rev. Fluid Mech.*, **14**(1), 189–212. https://doi.org/10.1146/annurev.fl.14.010182.001201

Liang, M., **Van Dyk, C.** and **Passalacqua, P.** (2016) Quantifying the patterns and dynamics of river deltas under conditions of steady forcing and relative sea level rise. *J. Geophys. Res. Earth Surface*, **121**, 465–496. https://doi.org/10.1002/2015JF003653

Loucks, D.P. (2019) Developed river deltas: are they sustainable? *Environ. Res. Lett.*, **14**, 113004.

Lwasa, S. (2015) A systematic review of research on climate change adaptation policy and practice in Africa and South Asia deltas. *Regional Environ. Change*, **15**, 815–824. https://doi.org/10.1007/s10113-014-0715-8

Martin, J., **Sheets, B.**, **Paola, C.** and **Hoyal, D.** (2009) Influence of steady base-level rise on channel mobility, shoreline migration, and scaling properties of a cohesive experimental delta. *J. Geophys. Res. Earth Surface*, **114**, 1–15. https://doi.org/10.1029/2008JF001142

Martin, J., **Cantelli, A.**, **Paola, C.**, **Blum, M.** and **Wolinsky, M.** (2011) Quantitative modelling of the evolution and geometry of incised valleys. *J. Sed. Res.*, **81**, 64–79. https://doi.org/10.2110/jsr.2011.5

Mikhailov, V.N. (1970) Hydrologic-morphometric characteristics of delta branches. *Stud. Rep. Hydrol.*, **9**, 146–158.

Mikhailov, V.N., **Magritsky, D.V.**, **Kravtsova, V.I.**, **Mikhailova, M.V.** and **Isupova, M.V.** (2012) The response of river mouths to large-scale variations in sea level and river runoff: case study of rivers flowing into the Caspian Sea. *Water Resour.*, **39**, 11–43. https://doi.org/10.1134/S0097807812010083

Mulder, T., **Syvitski, J.P.**, **Migeon, S.**, **Faugeres, J.C.** and **Savoye, B.** (2003) Marine hyperpycnal flows: initiation, behaviour and related deposits. A review. *Mar. Pet. Geol.*, **20**, 861–882. https://doi.org/10.1016/j.marpetgeo.2003.01.003

Olariu, C. and **Bhattacharya, J.P.** (2006) Terminal distributary channels and delta front architecture of river-dominated delta systems. *J. Sed. Res.*, **76**, 212–233. https://doi.org/10.2110/jsr.2006.026

Olariu, C., **Bhattacharya, J.P.**, **Leybourne, M.I.**, **Boss, S.K.** and **Stern, R.J.** (2012) Interplay between river discharge and topography of the basin floor in a hyperpycnal lacustrine delta. *Sedimentology*, **59**, 704–728. https://doi.org/10.1111/j.1365-3091.2011.01272.x

Okazaki, H. and **Masuda, F.** (1989) Arcuate and bird's foot deltas in the late Pleistocene Palaeo-Tokyo Bay. In: *Deltas: Sites and Traps for Fossil Fuels* (Eds Whateley, M.K.G. and Pickering, K.T.), Vol. **41**, pp. 129–138. *Geol. Soc. London Spec. Publ.* The Geological Society, London. https://doi.org/10.1144/GSL.SP.1989.041.01.10

Orton, G.J. and **Reading, H.G.** (1993) Variability of deltaic processes in terms of sediment supply, with particular emphasis on grain size. *Sedimentology*, **40**, 475–512. https://doi.org/10.1111/j.1365-3091.1993.tb01347.x

Overeem, I., **Kroonenberg, S.B.**, **Veldkamp, A.**, **Groenesteijn, K.**, **Rusakov, G.V.** and **Svitoch, A.A.** (2003) Small-scale stratigraphy in a large ramp delta: recent and Holocene sedimentation in the Volga delta, Caspian Sea. *Sed. Geol.*, **159**, 133–157. https://doi.org/10.1016/S0037-0738(02)00256-7

Passalacqua, P. (2017) The Delta Connectome: a network-based framework for studying connectivity in river deltas. *Geomorphology*, **277**, 50–62. https://doi.org/10.1016/j.geomorph.2016.04.001

Pezzetta, J.M. (1973) The Saint Clair River Delta; sedimentary characteristics and depositional environments. *J. Sed. Res.*, **43**, 168–187. https://doi.org/10.1306/74D72711-2B21-11D7-8648000102C1865D

Pulham, A.J. (1989) Controls on internal structure and architecture of sandstone bodies within Upper Carboniferous fluvial-dominated deltas, County Clare, western Ireland. In: *Deltas: Sites and Traps for Fossil Fuels* (Eds Whateley, M.K.G. and Pickering, K.T.), Vol. **41**, pp. 179–203. *Geol. Soc. London Spec. Publ.* The Geological Society, London. https://doi.org/10.1144/GSL.SP.1989.041.01.14

Richards, K. (2018) Studies in Caspian palynology: six million years of vegetation, climate and sea level change. Institute for Biodiversity and Ecosystem Dynamics, University of Amsterdam. 264p. https://hdl.handle.net/11245.1/333ad207-8303-4f5c-8ebb-b11d24fc8870

Riebeek, H. (2013) How to interpret a Satellite Image: Five Tips and Strategies. https://earthobservatory.nasa.gov/features/ColorImage/page1.php

Reading, H.G. and **Collinson, J.D.** (1996) Clastic coasts. In: *Sedimentary Environments: Processes, Facies and Stratigraphy* (Ed Reading, H.G.), 3rd edn, pp. 154–231. *Blackwell Science*, Oxford.

Reynolds, A.D. (1996) Paralic successions. In: *Sequence Stratigraphy* (Eds Emery, D. and Myers, K.), pp. 134–177. Blackwell Science, Oxford.

Reynolds, A.D. (2017) Paralic reservoirs. In: *Deltas: Sites and Traps for Fossil Fuels* (Eds Hampson, G.J., Reynolds, A.D., Kostic, B. and Wells, M.R.), Vol. **444**, pp. 7–34. *Geol. Soc. London Spec. Publ.* The Geological Society, London. https://doi.org/10.1144/SP444.10

Roberts, H.H. (1998) Delta switching: early responses to the Atchafalaya River diversion. *J. Coastal Res.*, **14**, 882–899.

Rosa, M.L.C.C., **Hoyal, D.C.**, **Barboza, E.G.**, **Fedele, J.** and **Abreu, V.S.** (2016) River-dominated deltas: upscaling autogenic and allogenic processes observed in laboratory experiments to field examples of small deltas in southern Brazil. In: *Autogenic Dynamics and Self-organization in Sedimentary Systems* (Eds Budd, D.A., Hajek, E.A. and Purkis, S.J.), Vol. **106**, pp. 176–197. *SEPM Spec. Publ.* SEPM, Tulsa. https://doi.org/10.2110/sepmsp.106.13

Rossi, V.M., **Kim, W.**, **Leva López, J.**, **Edmonds, D.**, **Geleynse, N.**, **Olariu, C.**, **Steel, R.J.**, **Hiatt, M.** and **Passalacqua, P.** (2016) Impact of tidal currents on delta-channel deepening, stratigraphic architecture, and sediment bypass beyond the shoreline. *Geology*, **44**, 927–930. https://doi.org/10.1130/G38334.1

Rowland, J.C., **Lepper, K.**, **Dietrich, W.E.**, **Wilson, C.J.** and **Sheldon, R.** (2005) Tie channel sedimentation rates, oxbow formation age and channel migration rate from optically stimulated luminescence (OSL) analysis of floodplain deposits. *Earth Surf. Process. Landforms*, **30**, 1161–1179. https://doi.org/10.1002/esp.1268

Rowland, J.C. (2007) *Tie channels*, p. 166. University of California, Berkeley.

Rowland, J.C., **Dietrich, W.E.**, **Day, G.** and **Parker, G.** (2009) Formation and maintenance of single-thread tie channels entering floodplain lakes: Observations from three diverse river systems. *J. Geophys. Res. Earth Surface*, **114**, 1–19. https://doi.org/10.1029/2008JF001073

Rowland, J.C., **Dietrich, W.E.** and **Stacey, M.T.** (2010) Morphodynamics of subaqueous levee formation: insights into river mouth morphologies arising from experiments. *J. Geophys. Res. Earth Surface*, **115**, 1–20. https://doi.org/10.1029/2010JF001684

Schneider, P. and **Asch, F.** (2020) Rice production and food security in Asian Mega deltas – a review on characteristics, vulnerabilities and agricultural adaptation options to cope with climate change. *J. Agronomy Crop Sci.*, **206**, 491–503. https://doi.org/10.1111/jac.12415

Seybold, H., **Andrade, J.S.** and **Herrmann, H.J.** (2007) Modelling river delta formation. *Proc. Natl Acad. Sci.*, **104**, 16804–16809. www.pnas.org/cgi/doi/10.1073/pnas.0705265104

Shaw, J.B., **Miller, K.** and **McElroy, B.** (2018) Island formation resulting from radially symmetric flow

expansion. *J. Geophys. Res. Earth Surf.*, **123**, 363–383. https://doi.org/10.1002/2017jf004464

Shaw, J.B. and **Mohrig, D.** (2014) The importance of erosion in distributary channel network growth, Wax Lake Delta, Louisiana, USA. *Geology*, **42**, 31–34. https://doi.org/10.1130/G34751.1

Scheelbeek, P.F., **Chowdhury, M.A.**, **Haines, A.**, **Alam, D.S.**, **Hoque, M.A.**, **Butler, A.P.**, **Khan, A.E.**, **Mojumder, S.K.**, **Blangiardo, M.A.**, **Elliott, P.** and **Vineis, P.** (2017) Drinking water salinity and raised blood pressure: evidence from a cohort study in coastal Bangladesh. *Environ. Health Perspect.*, **125**, 057007, 1–7. https://doi.org/10.1289/EHP659

Stride, A.H. (1982) *Offshore Tidal Sands*, p. 222. Springer, Dordrecht. https://doi.org/10.1007/978-94-009-5726-8_5

Syvitski, J.P. (2008) Deltas at risk. *Sustainability Sci.*, **3**, 23–32. https://doi.org/10.1007/s11625-008-0043-3

Syvitski, J.P., **Kettner, A.J.**, **Overeem, I.**, **Hutton, E.W.**, **Hannon, M.T.**, **Brakenridge, G.R.**, **Day, J.**, **Vörösmarty, C.**, **Saito, Y.**, **Giosan, L.** and **Nicholls, R.J.** (2009) Sinking deltas due to human activities. *Nat. Geosci.*, **2**, 681–686. https://doi.org/10.1038/ngeo629

Tanner, W.F. (1971) Numerical estimates of ancient waves, water depth and fetch. *Sedimentology*, **16**, 71–88. https://doi.org/10.1111/j.1365-3091.1971.tb00219.x

Tessler, Z.D., **Vörösmarty, C.J.**, **Grossberg, M.**, **Gladkova, I.**, **Aizenman, H.**, **Syvitski, J.P.M.** and **Foufoula-Georgiou, E.** (2015) Profiling risk and sustainability in coastal deltas of the world. *Science*, **349**, 638–643. https://doi.org/10.1126/science.aab3574

Tomanka, G.D. (2013) *Morphology, Mechanisms, and Processes for the formation of a non-bifurcating fluvial-deltaic channel prograding into Grapevine Reservoir, Texas*, p. 113. University of Texas, Arlington.

Turner, J.S. (1979) *Buoyancy Effects in Fluids*, p. 267. Cambridge University Press, Cambridge.

Turner, B.R. and **Tester, G.N.** (2006) The Table Rocks Sandstone: a fluvial, friction-dominated lobate mouth bar sandbody in the Westphalian B Coal Measures, NE England. *Sed. Geol.*, **190**, 97–119. https://doi.org/10.1016/j.sedgeo.2006.05.007

Tye, R.S. and **Hickey, J.J.** (2001) Permeability characterization of distributary mouth bar sandstones in Prudhoe Bay field, Alaska: how horizontal cores reduce risk in developing deltaic reservoirs. *AAPG Bull.*, **85**, 459–475. https://doi.org/10.1306/8626C91F-173B-11D7-8645000102C1865D

Van Heerden, I.L. and **Roberts, H.H.** (1988) Facies development of Atchafalaya Delta, Louisiana: a modern bayhead delta. *AAPG Bull.*, **72**, 439–453. https://doi.org/10.1306/703C8EB1-1707-11D7-8645000102C1865D

Van Heerden, I.L., **Roberts, H.H.**, **Penland, S.** and **Cunningham, R.H.** (1991) Subaerial delta development, eastern Atchafalaya Bay, Louisiana. In: *Coastal Depositional Systems in the Gulf of Mexico, Quaternary Framework and Environmental Issues. 12th Annual Research Conference of the Gulf Coast Section SEPM Foundation*, pp. 271–277. SEPM, Tulsa.

Velpuri, N.M., **Senay, G.B.** and **Asante, K.O.** (2012) A multi-source satellite data approach for modelling Lake Turkana water level: calibration and validation using satellite altimetry data. *Hydrol. Earth Syst. Sci.*, **16**, 1–18. https://doi.org/10.5194/hess-16-1-2012

Waldrop, W.R. and **Farmer, R.C.** (1974) Three-dimensional computation of buoyant plumes. *J. Geophys. Res.*, **79**, 1269–1276. https://doi.org/10.1029/JC079i009p01269

Wale, A. (2008) *Hydrological Balance of Lake Tana Upper Blue Nile Basin, Ethiopia*, p. 94. International Institute for Geo-information Science and Earth Observation, The Netherlands.

Welder, F.A. (1955) *Deltaic Processes in Cubit's Gap Area Plaquemines Parish, Louisiana*, p. 149. Louisiana State University, Louisiana.

Wellner, R., **Beaubouef, R.**, **Van Wagoner, J.**, **Roberts, H.** and **Sun, T.** (2005) Jet-plume depositional bodies – the primary building blocks of Wax Lake Delta. *Trans. Gulf Coast Assoc. Geol. Soc.*, **55**, 867–909.

Whateley, M.K.G. and **Pickering, K.T.** (1989) Deltas – sites and traps for fossil fuels. *Geol. Soc. London Spec. Publ.*, **41**, 360.

Wolinsky, M.A., **Edmonds, D.A.**, **Martin, J.** and **Paola, C.** (2010) Delta allometry: growth laws for river deltas. *Geophys. Res. Lett.*, **37**, 1–6. https://doi.org/10.1029/2010GL044592

Wright, L.D., **Coleman, J.M.** and **Erickson, M.W.** (1974) *Analysis of Major River Systems and Their Deltas: Morphologic and Process Comparisons*, p. 114. Louisiana State University, Coastal Studies Institute, Louisiana.

Wright, L.D. and **Coleman, J.M.** (1974) Mississippi River mouth processes: effluent dynamics and morphologic development. *J. Geol.*, **82**, 751–778. https://doi.org/10.1086/628028

Wright, L.D. (1977) Sediment transport and deposition at river mouths: a synthesis. *Geol. Soc. Am. Bull.*, **88**, 857–868. https://doi.org/10.1130/0016-7606(1977)88<857:STADAR>2.0.CO;2

Zeng, H., **Zhu, X.** and **Zhu, R.** (2013) New insights into seismic stratigraphy of shallow-water progradational sequences: sub-seismic clinoforms. *Interpretation*, **1**, SA35-SA51. https://doi.org/10.1190/INT-2013-0017.1

Manuscript received 27 March 2021; revision accepted 12 May 2022

